惠州强子谱仪HHaS合作组年会，
惠州，11月28-30日，2025

Hypernuclear production and hyperon-nucleon interaction in dense baryonic matter at HHaS

Zhao-Qing Feng (冯兆庆)

School of Physics and Optoelectronics, South China University of Technology, Guangzhou

***Email: fengzhq@scut.edu.cn**

Outline

- Hadrons (meson, antiproton) induced reactions at HHaS
- Cluster, hyperon and hypercluster production via heavy-ion collisions (HICs) for neutron-star matter properties
- LQMD transport model
- Hyperon-nucleon interaction in dense nuclear matter via HICs

^{56}Fe 800 MeV/nucleon on ^{208}Pb

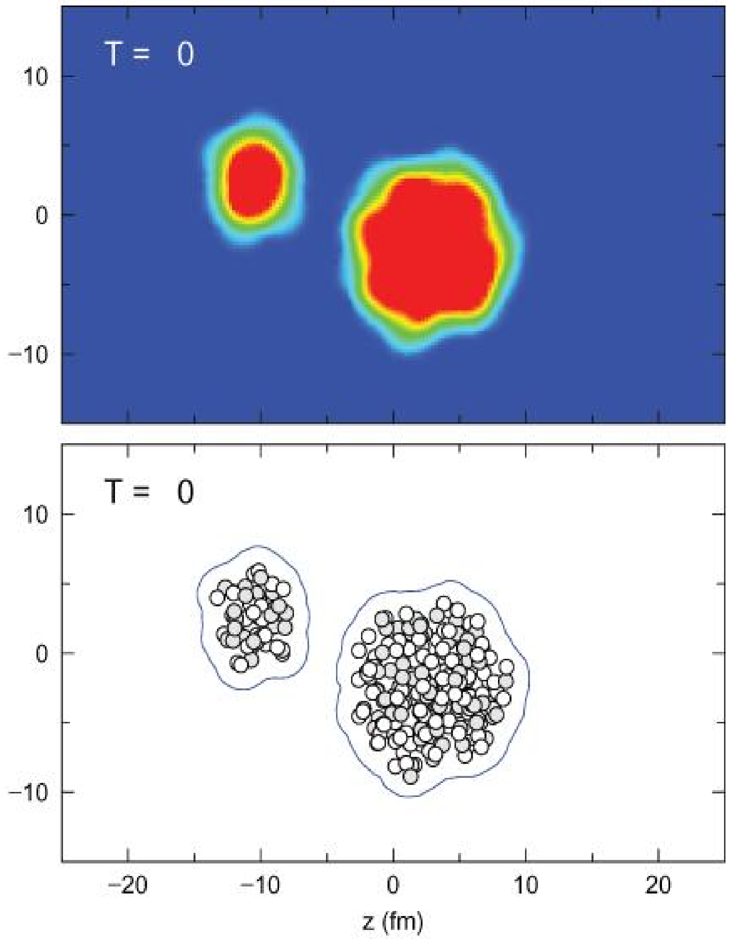

I. Hadrons (meson, antiproton) induced reactions at HHaS

PHYSICAL REVIEW C **94**, 054617 (2016)

Nuclear fragmentation and charge-exchange reactions induced by pions in the Δ-resonance region

Zhao-Qing Feng*
Institute of Modern Physics, Chinese Academy of Sciences, Lanzhou 730000, People's Republic of China
(Received 5 September 2016; revised manuscript received 11 October 2016; published 18 November 2016)

The dynamics of the nuclear fragmentations and the charge exchange reactions in pion-nucleus collisions near the Δ(1232) resonance energies has been investigated within the Lanzhou quantum molecular dynamics transport model. An isospin-, momentum-, and density-dependent pion-nucleon potential is implemented in the model, which influences the pion dynamics, in particular the kinetic energy spectra, but weakly impacts the fragmentation mechanism. The absorption process in pion-nucleon collisions to form the Δ(1232) resonance dominates the heating mechanism of the target nucleus. The excitation energy transferred to the target nucleus increases with the pion kinetic energy and is similar for both π^-- and π^+-induced reactions. The magnitude of fragmentation of the target nucleus weakly depends on the pion energy. The isospin ratio in the pion double-charge exchange is influenced by the isospin ingredient of target nucleus.

DOI: 10.1103/PhysRevC.94.054617

中国科学: 物理学 力学 天文学 2020 年 第 50 卷 第 11 期: 112010
SCIENTIA SINICA Physica, Mechanica & Astronomica physcn.scichina.com
《中国科学》杂志社 SCIENCE CHINA PRESS
CrossMark
进 展 强流重离子加速器及其科学研究专题

基于HIAF集群的高强度缪子、反质子次级束产生及其物理研究展望

孙志宇[1,2*], 陈良文[1], 蔡汉杰[1], 李亮[3,4], 尤郑昀[5], 袁野[2,6], 王莹[5], 谢聚军[1,2], 冯兆庆[7], 王世陶[1,2]

1. 中国科学院近代物理研究所, 兰州 730000;
2. 中国科学院大学, 北京 100049;
3. 上海交通大学物理与天文学院, 上海 200240;
4. 上海市粒子物理和宇宙学重点实验室, 上海 200240;
5. 中山大学物理学院, 广州 510275;
6. 中国科学院高能物理研究所, 北京 100049;
7. 华南理工大学物理与光电学院, 广州 510641

*联系人, E-mail: sunzhy@impcas.ac.cn

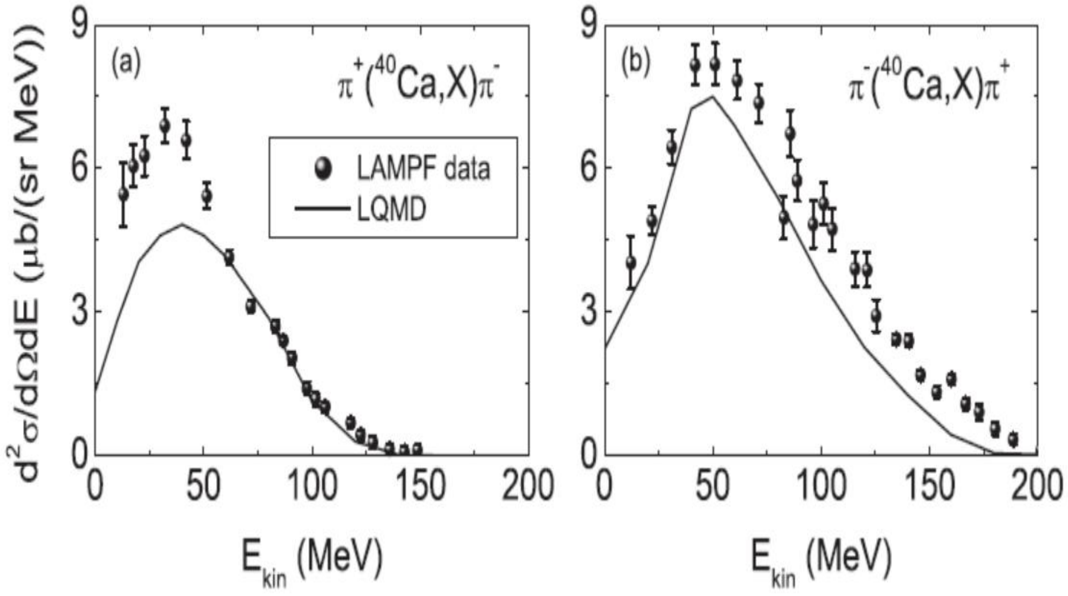

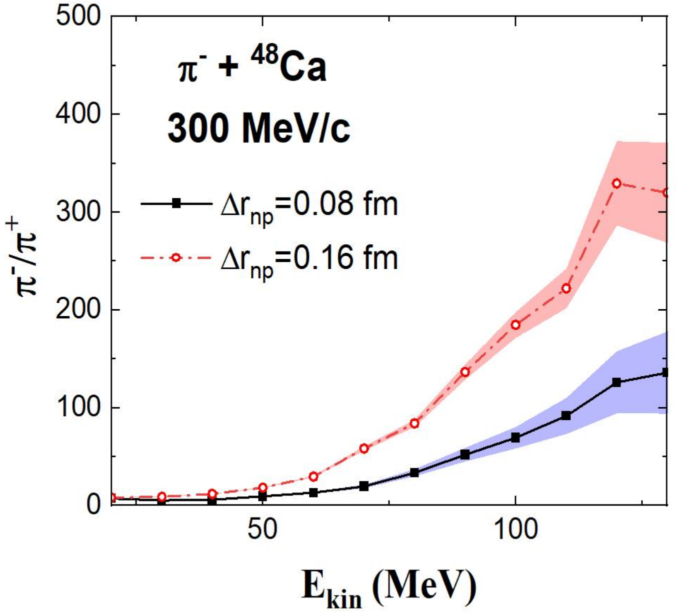

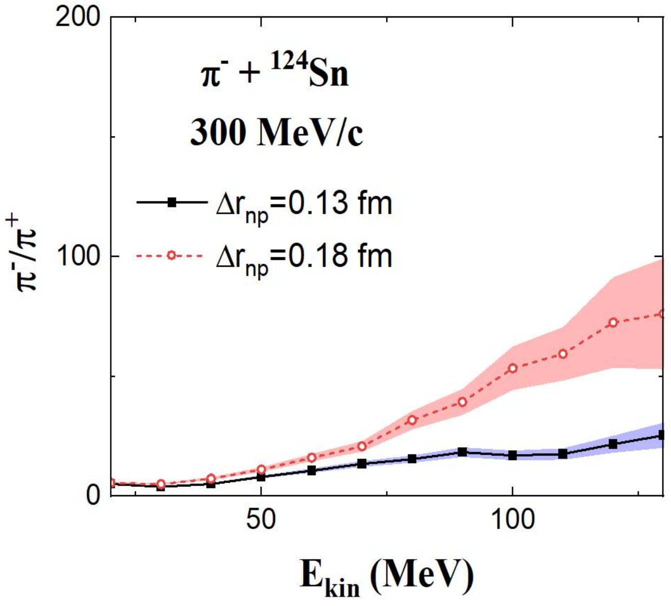

The neutron-skin thickness from antiproton and meson induced reactions

Zhao-Qing Feng, PRC 94, 054617 (2016)
Ban Zhang and Zhao-Qing Feng, PRC 111, 014607 (2025)

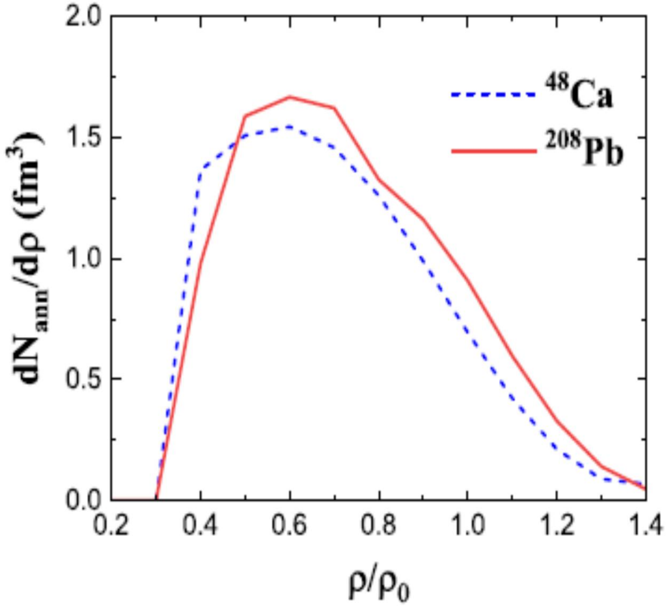

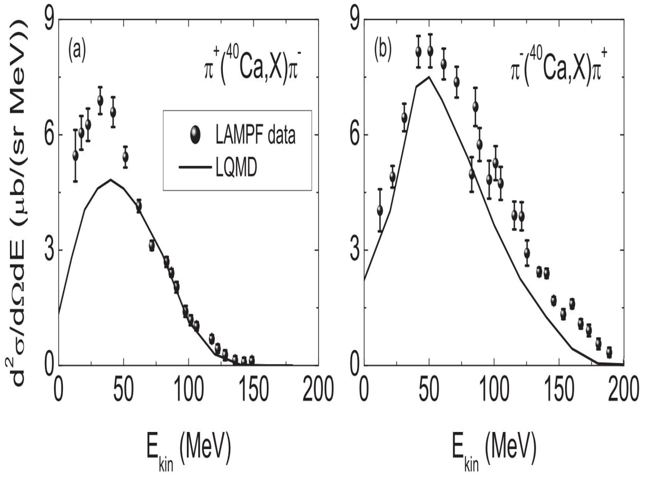

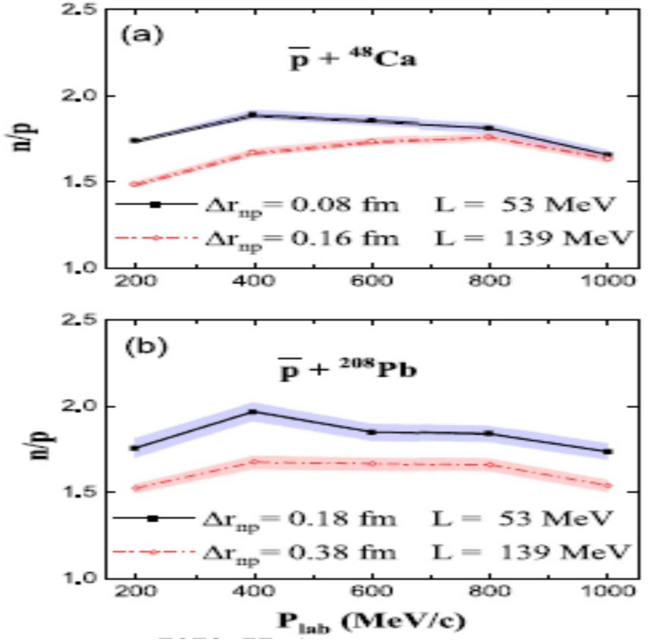

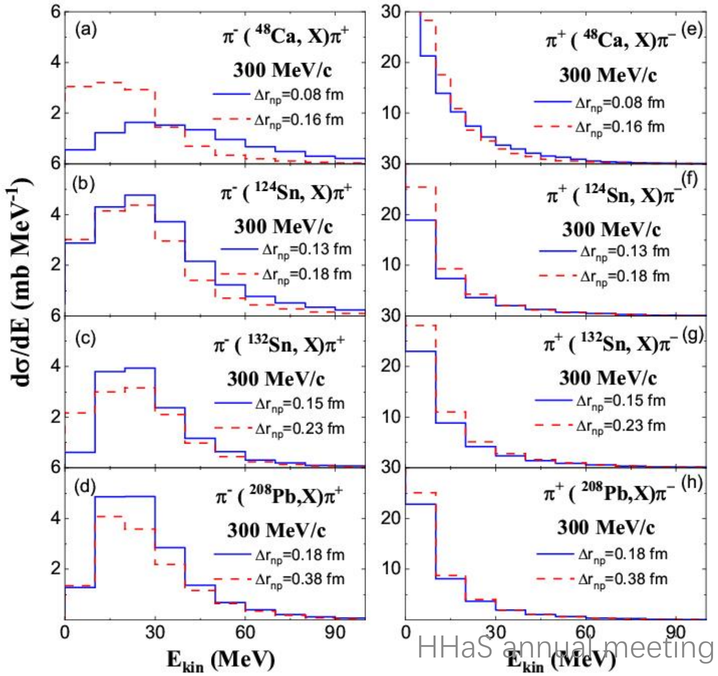

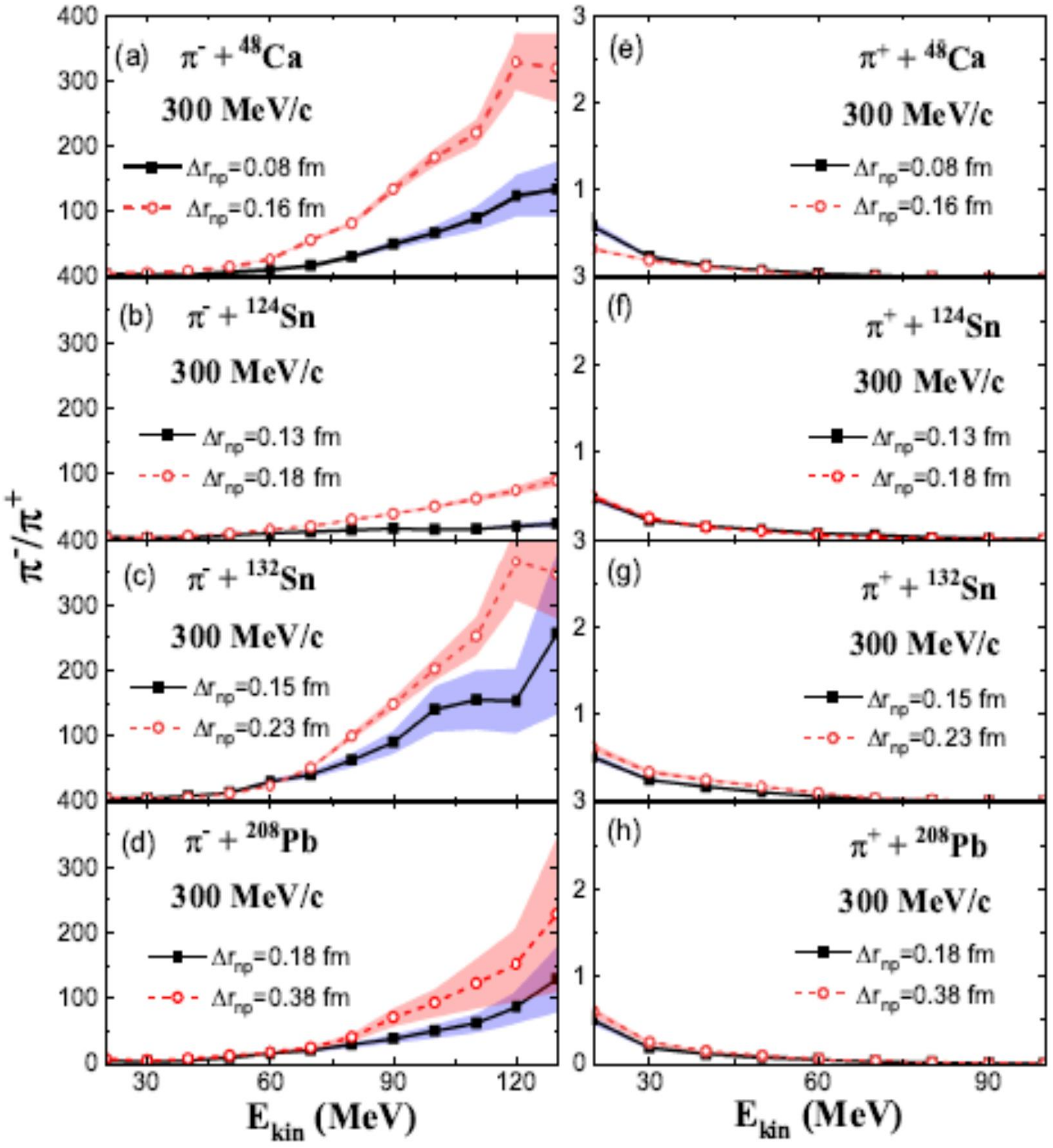

Neutron-skin thickness induced by antiprotons

PUMA， Proton Unstable Matter Annihilation at CERN

Z. Q. Feng, Phys. Rev. C 89, 044617 (2014); PRC 93, 041601(R) (2016); PRC 101, 064601 (2020); Ban Zhang and Zhao-Qing Feng, PRC 111, 014607 (2025).

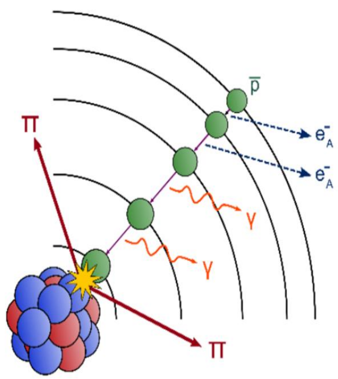

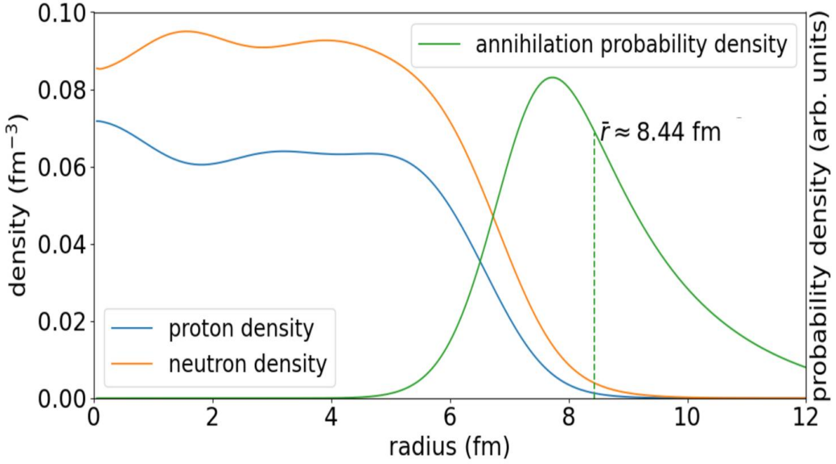

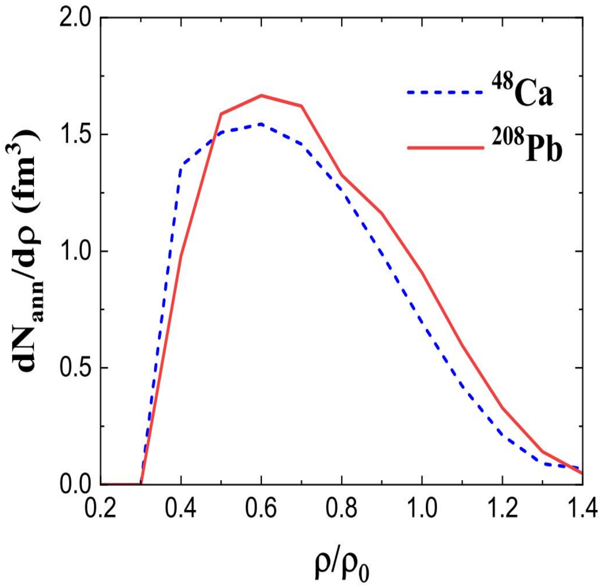

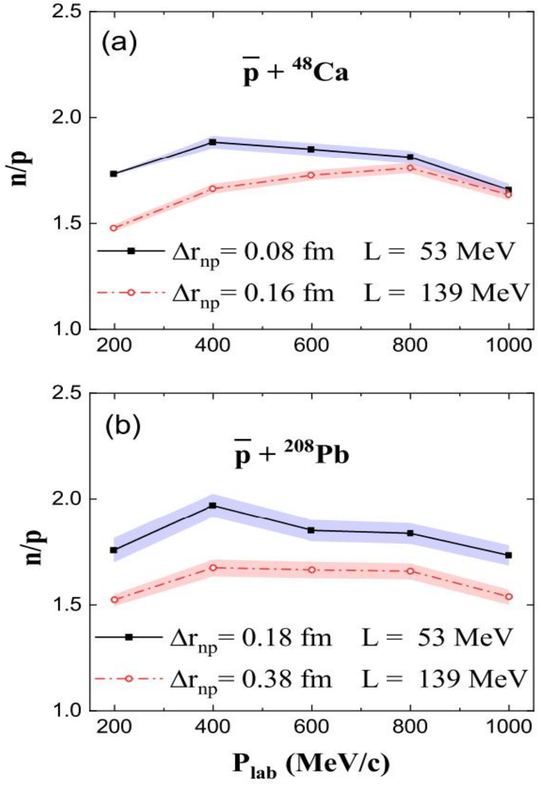

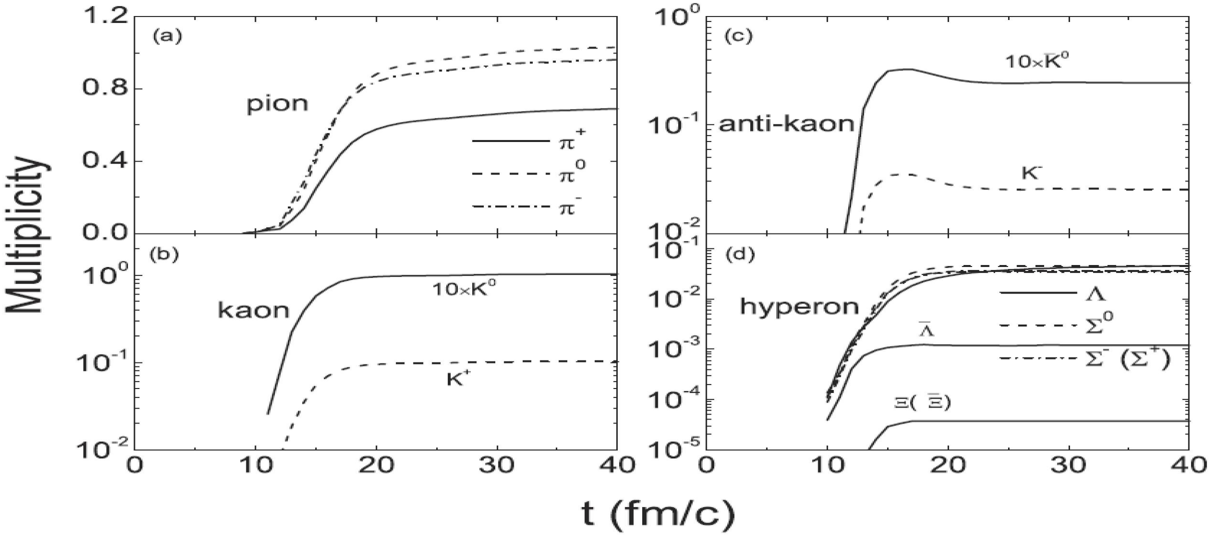

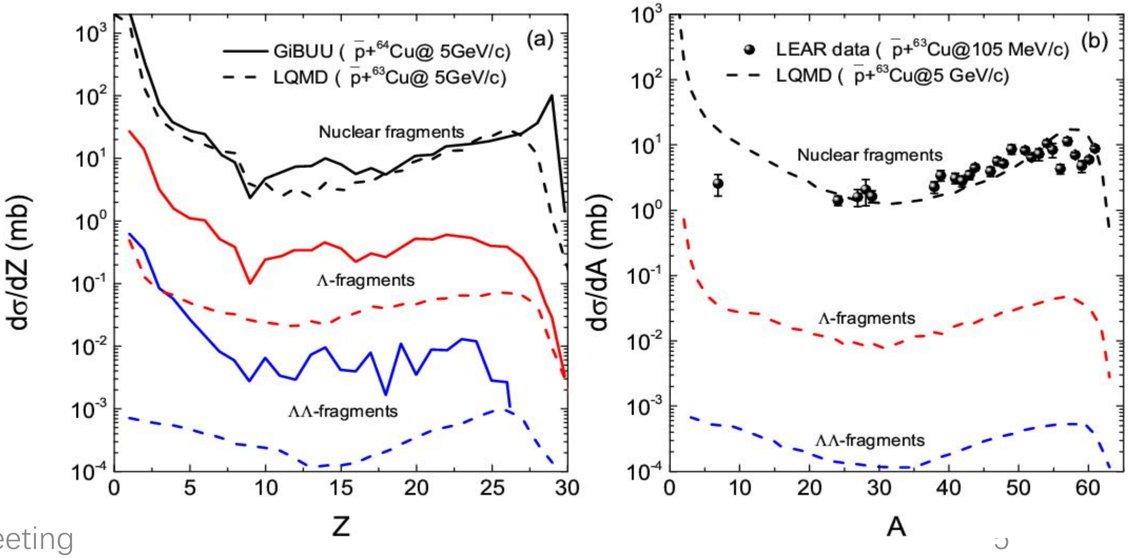

The data from LEAR facility at CERN. J. Jastrzebski *et al.*, Phys. Rev. C 47, 216 (1993)

II. Cluster, hyperon and hypercluster production via heavy-ion collisions (HICs) for neutron-star matter properties

1. Strange particle production in hadron-hadron collisions

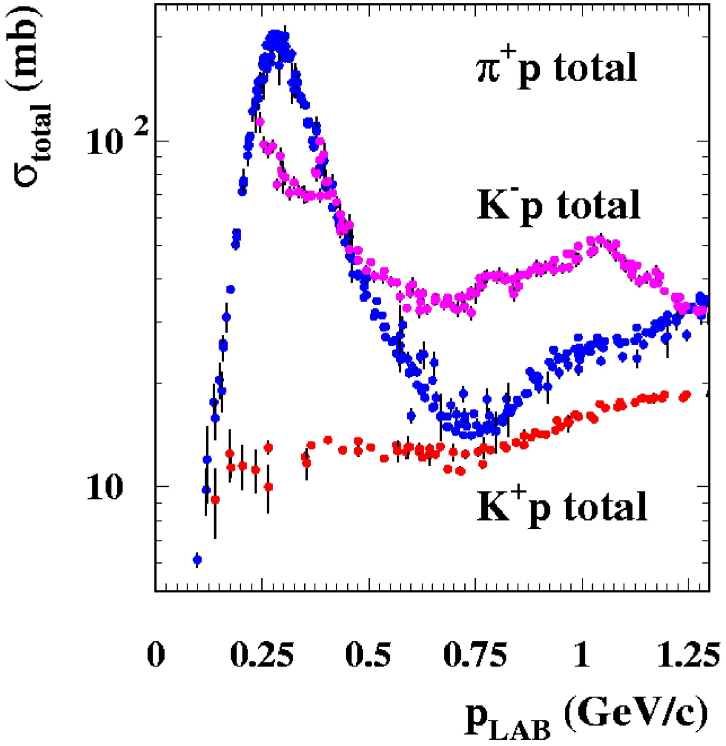

mean free path at ρ_0:

$\lambda(\pi) = 0.3$ fm

$\lambda(K^+) = 5$ fm

$\lambda(K^-) = 0.8$ fm

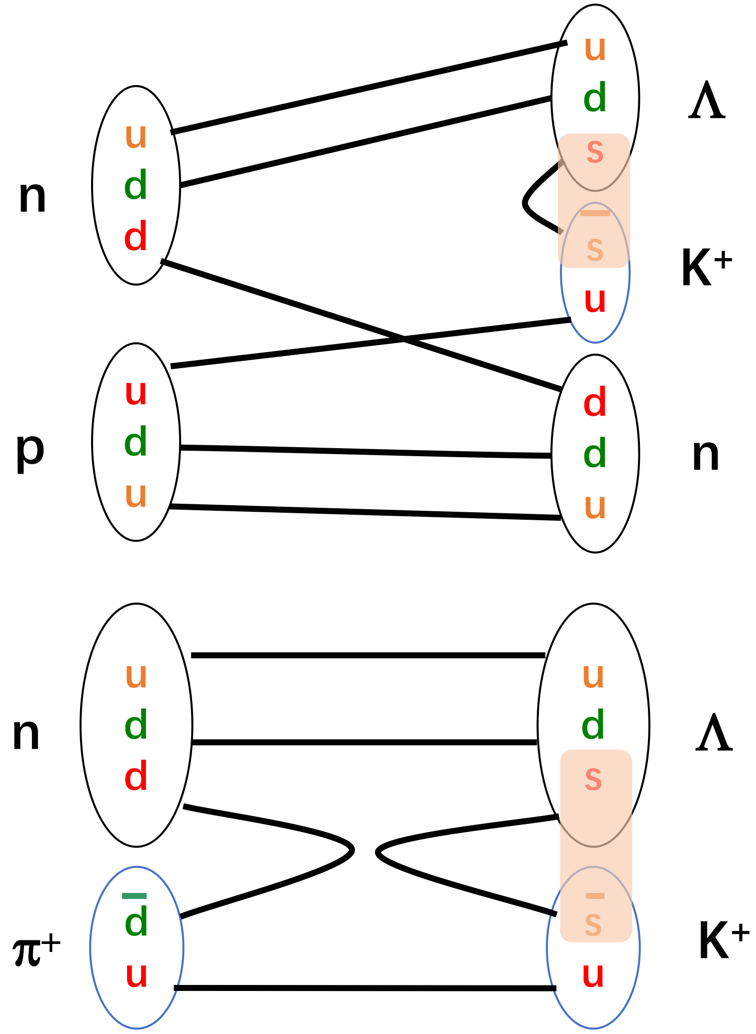

科学通报 2018 年 第 63 卷 第 8 期：735～744
论 文
SCIENCE CHINA PRESS

中高能重离子碰撞中奇异粒子产生和超核形成机制

冯兆庆

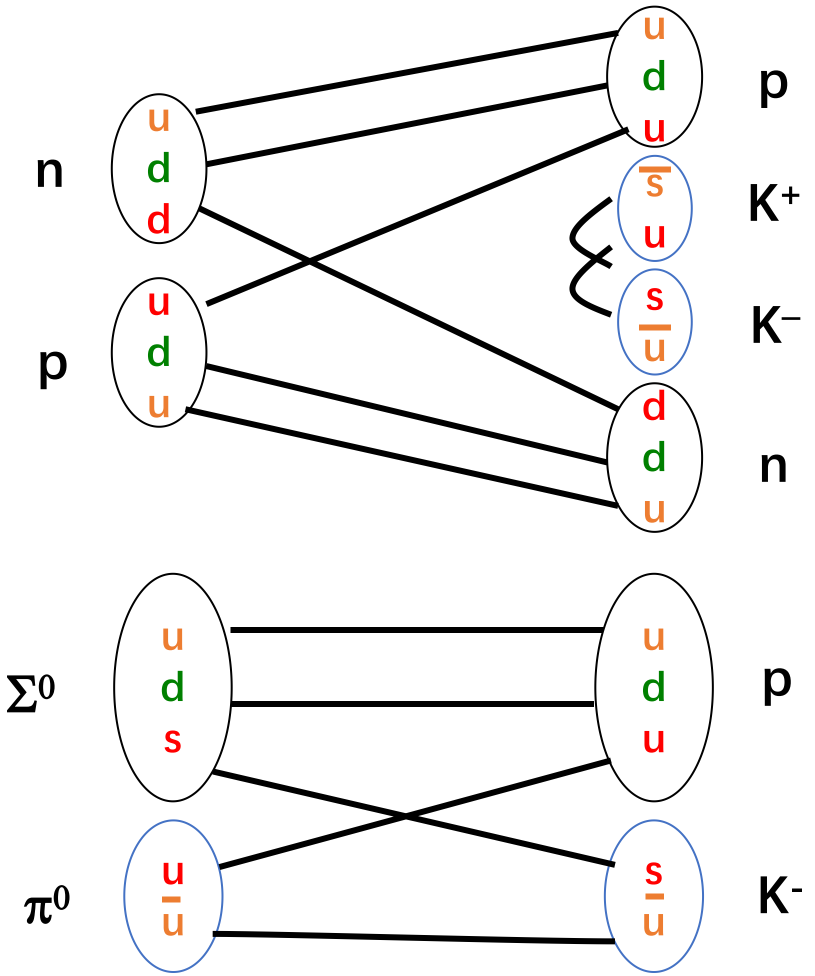

2. Cluster production in heavy-ion collisions

Available online at www.sciencedirect.com
ScienceDirect
Nuclear Physics A 848 (2010) 366–427
NUCLEAR PHYSICS A
www.elsevier.com/locate/nuclphysa

Experiments:
SSC and CSR(HIRFL), INDRA (GANIL), CHIMERA (LNS), NSCL (MSU), FOPI and HADES (GSI) …

Cluster production measurement at FOPI

Multiplicities and charge balance for Au + Au at $E/A = 0.15$ GeV and $b_0 < 0.15$.

$Z = 1$	59.9 ± 3.0	p	24.1 ± 1.2	$Z = 2$	25.0 ± 1.8	^{3}He	8.4 ± 0.9
		d	20.4 ± 1.4			^{4}He	16.6 ± 1.7
		t	15.1 ± 1.5				
		Li	5.0 ± 0.5	Be	1.69 ± 0.17		
		B	1.44 ± 0.15	C	0.90 ± 0.09		
		N	0.50 ± 0.05	O	0.26 ± 0.03		

Multiplicities and charge balance for Ni + Ni at $E/A = 0.25$ GeV and $b_0 < 0.15$.

$Z = 1$	34.9 ± 1.8	p	19.2 ± 1.0	$Z = 2$	9.0 ± 0.7	^{3}He	3.24 ± 0.33
		d	10.5 ± 0.8			^{4}He	5.79 ± 0.58
		t	5.1 ± 0.5				
		Li	0.91 ± 0.09	Be	0.26 ± 0.03		
		B	0.10 ± 0.01				

Systematics of central heavy ion collisions in the 1*A* GeV regime

FOPI Collaboration

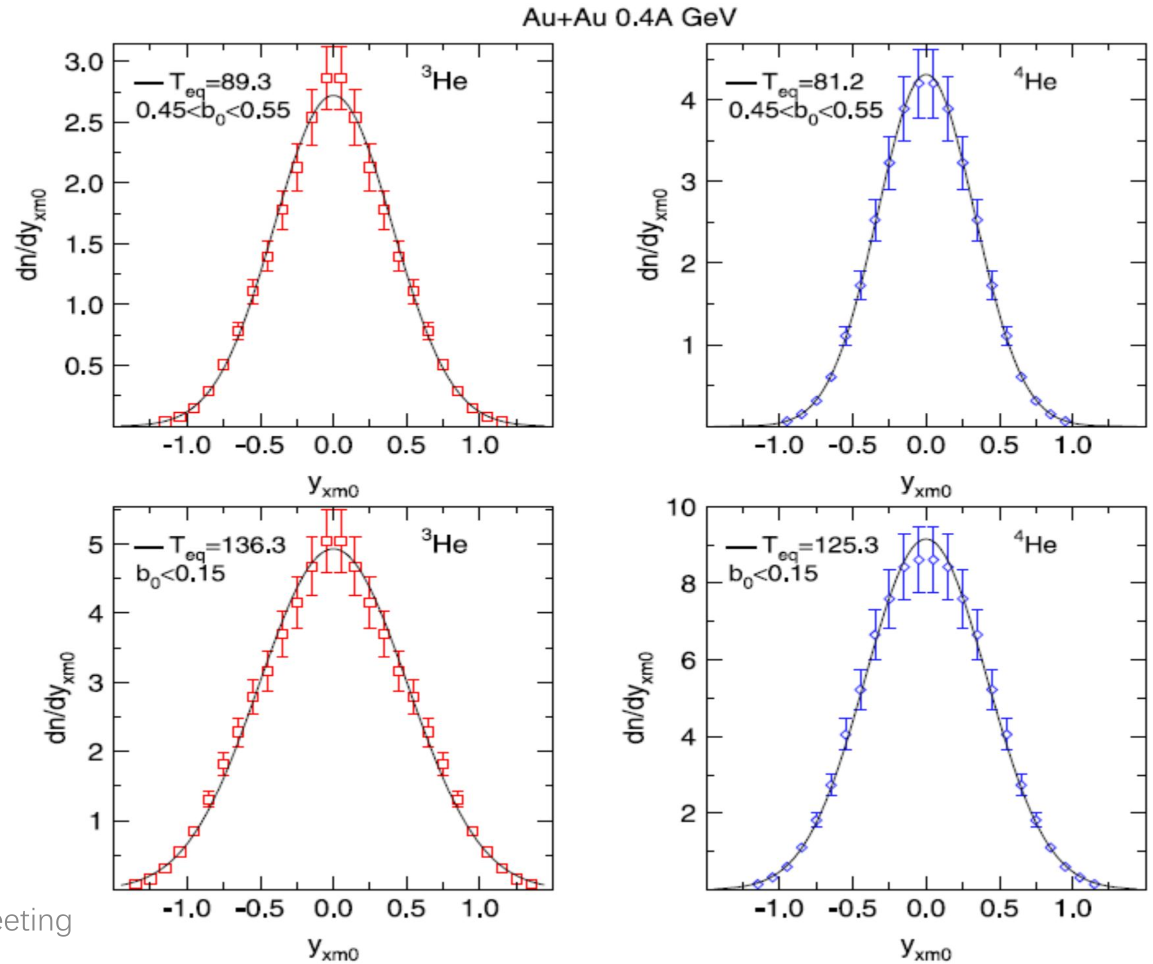

Cluster production measurement

PHYSICAL REVIEW C **107**, 044614 (2023)

Featured in Physics

Examination of cluster production in excited light systems at Fermi energies from new experimental data and comparison with transport model calculations

C. Frosin,[1,2,*] S. Piantelli,[2] G. Casini,[2] A. Ono,[3] A. Camaiani,[4] L. Baldesi,[2] S. Barlini,[1,2] B. Borderie,[5] R. Bougault,[6] C. Ciampi,[1,2] M. Cicerchia,[7] A. Chbihi,[8] D. Dell'Aquila,[9,10] J. A. Dueñas,[11] D. Fabris,[12] Q. Fable,[13] J. D. Frankland,[8] T. Génard,[8] F. Gramegna,[7] D. Gruyer,[6] M. Henri,[8] B. Hong,[14,15] M. J. Kweon,[16] S. Kim,[17] A. Kordyasz,[18] T. Kozik,[19] I. Lombardo,[20,21] O. Lopez,[6] T. Marchi,[7] K. Mazurek,[22] S. H. Nam,[14,15] J. Lemarié,[8] N. LeNeindre,[6] P. Ottanelli,[2] M. Parlog,[6,23] J. Park,[14,15] G. Pasquali,[1,2] G. Poggi,[1,2] A. Rebillard-Soulié,[6] B. H. Sun,[24] A. A. Stefanini,[1,2] S. Terashima,[24] S. Upadhyaya,[19] S. Valdré,[2] G. Verde,[20,13] E. Vient,[6] and M. Vigilante[25,26]
(INDRA-FAZIA Collaboration)

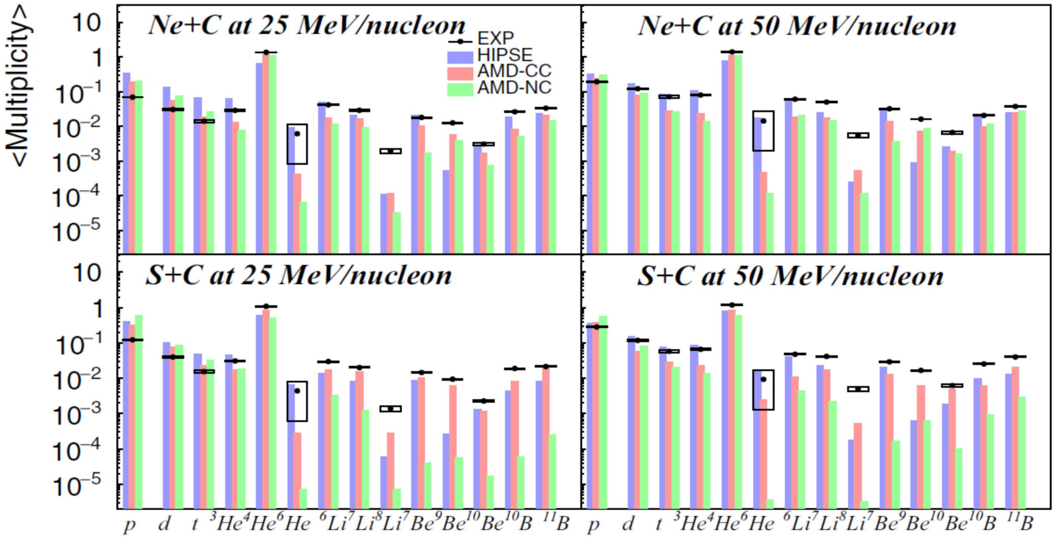

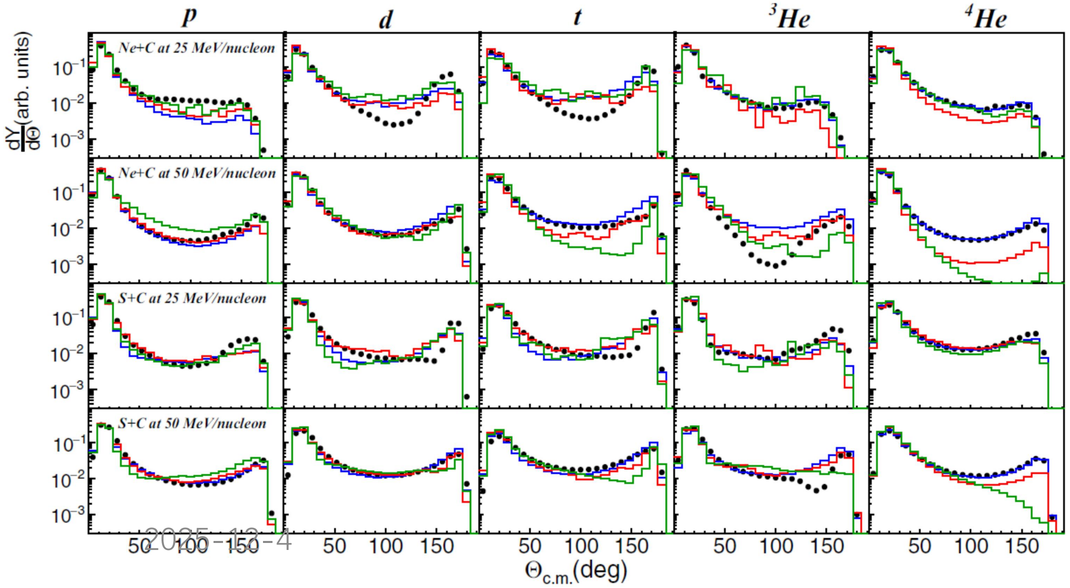

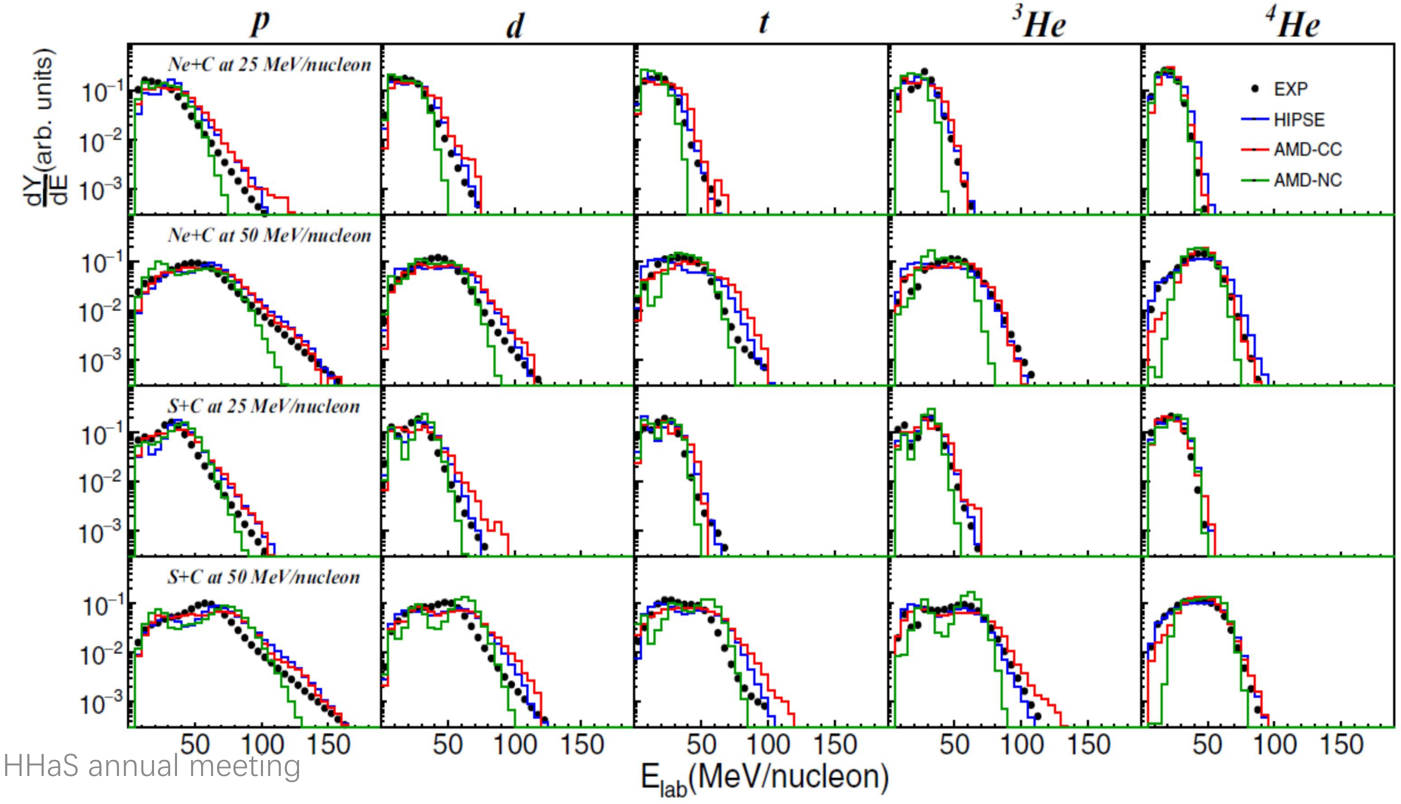

3. Strange particle production in HICs

C. Hartnack et al. / Physics Reports 510 (2012) 119–200

K+ production

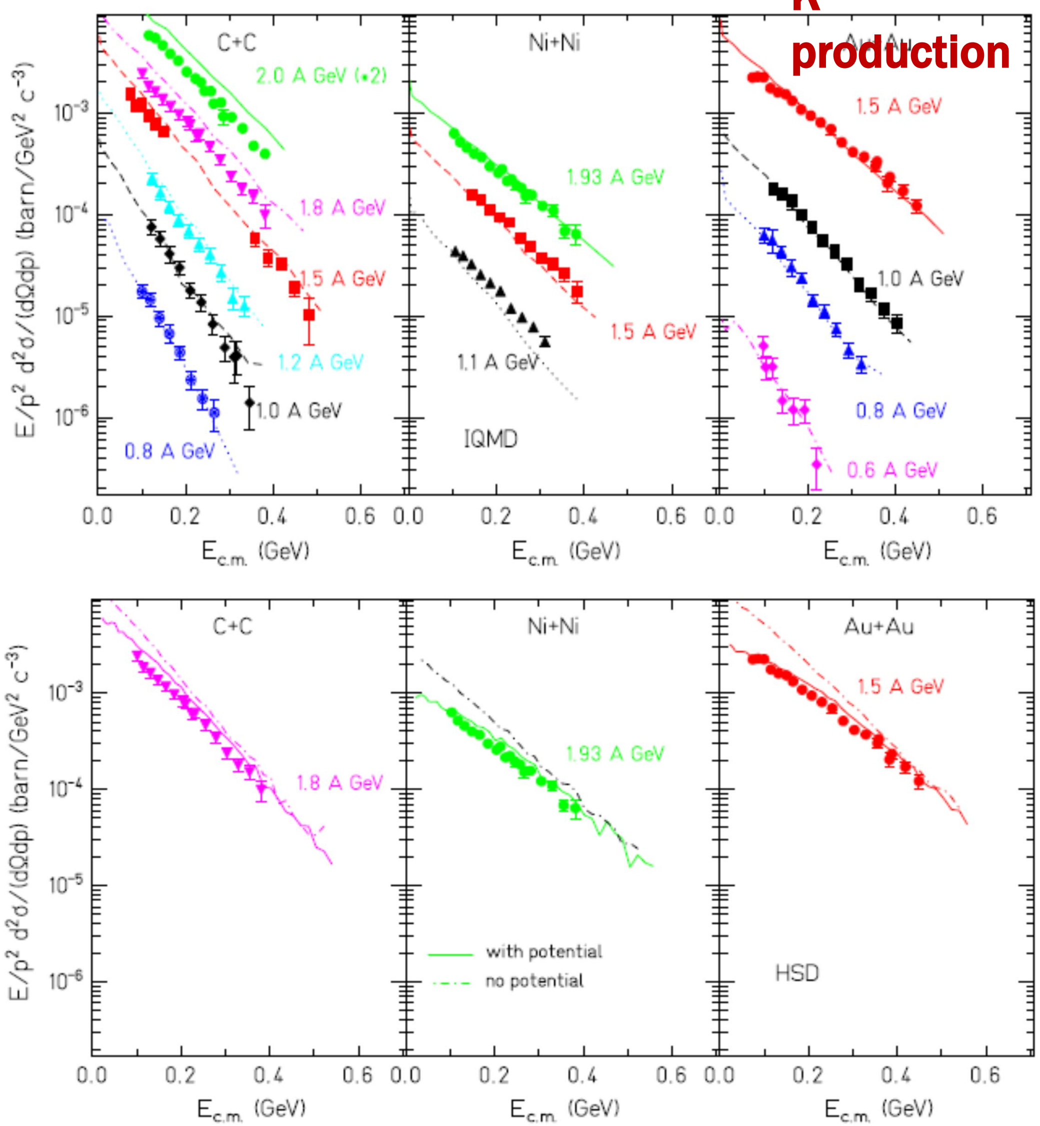

The ratio of K^-/K^+ in HICs of $^{12}C + {}^{12}C$ ($^{197}Au + {}^{197}Au$) at 1.8*A* GeV and proton beams at 2.5 GeV

(Z. Q. Feng et al., Phys. Rev. C 90, 064604 (2014))

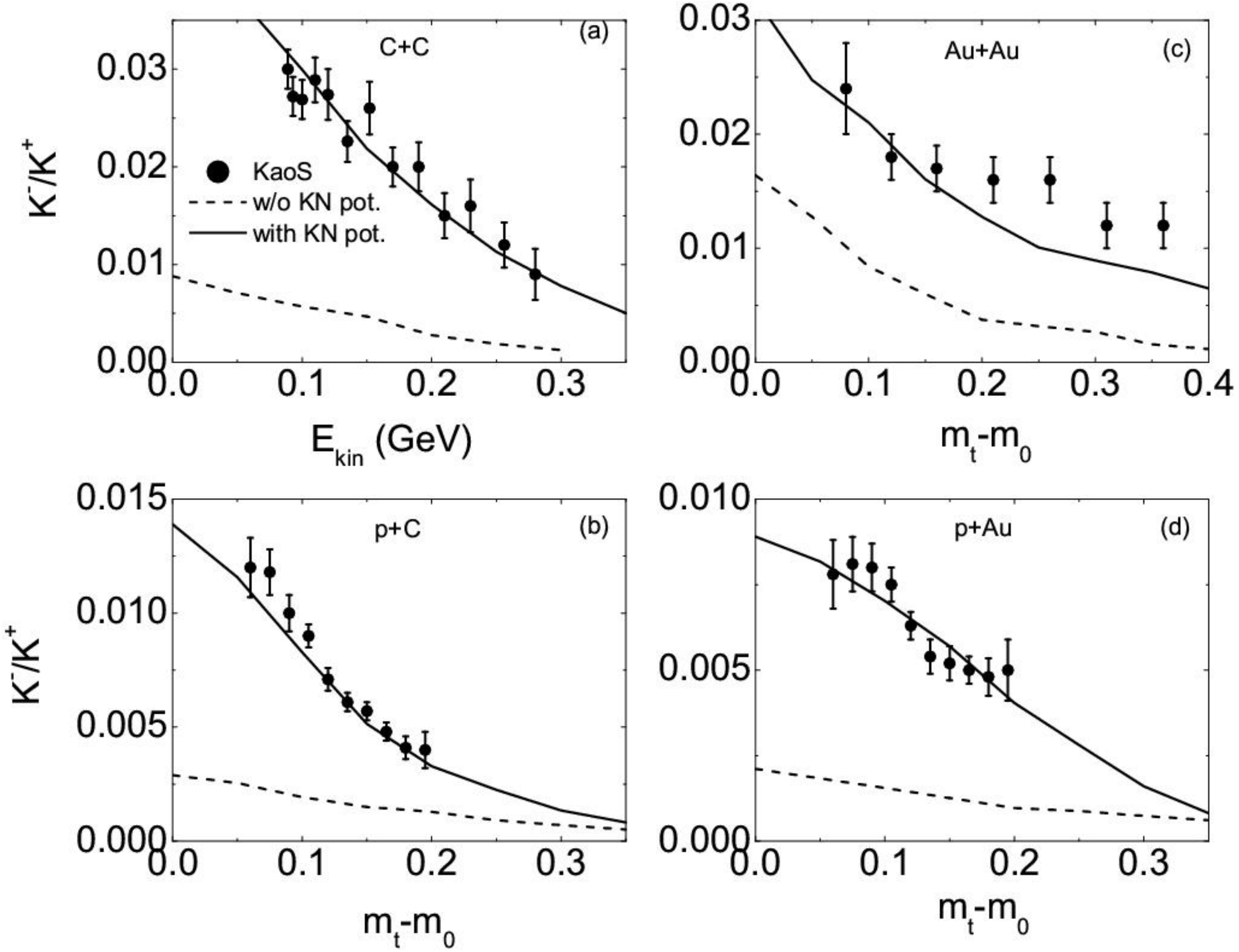

$V_{K+}(\rho_0)$= 28 MeV, $V_{K-}(\rho_0)$= -100 MeV

Kaon and hyperon production in HICs (yields, invariant energy spectra, collective flows)

ZQF, Phys. Rev. C 82 (2010) 057901; Phys. Rev. C 87 (2013) 064605; Ding-Chang Zhang et al., Chin. Phys. Lett. 38 (2021) 092501

^{197}Au+^{197}Au@1.5*A*GeV

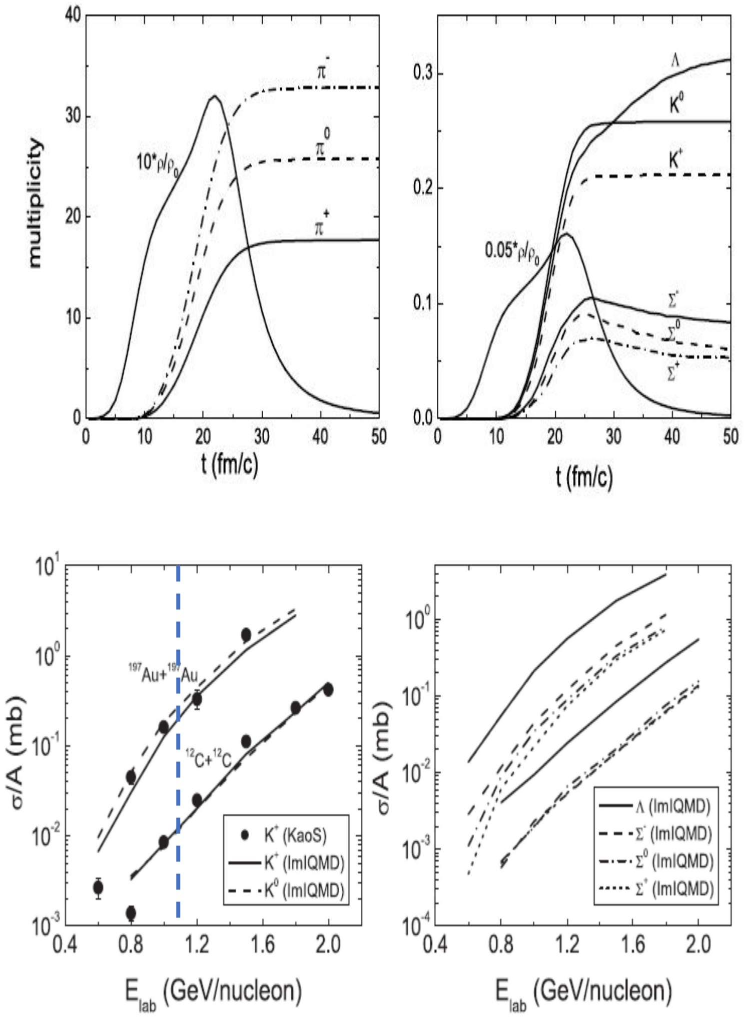

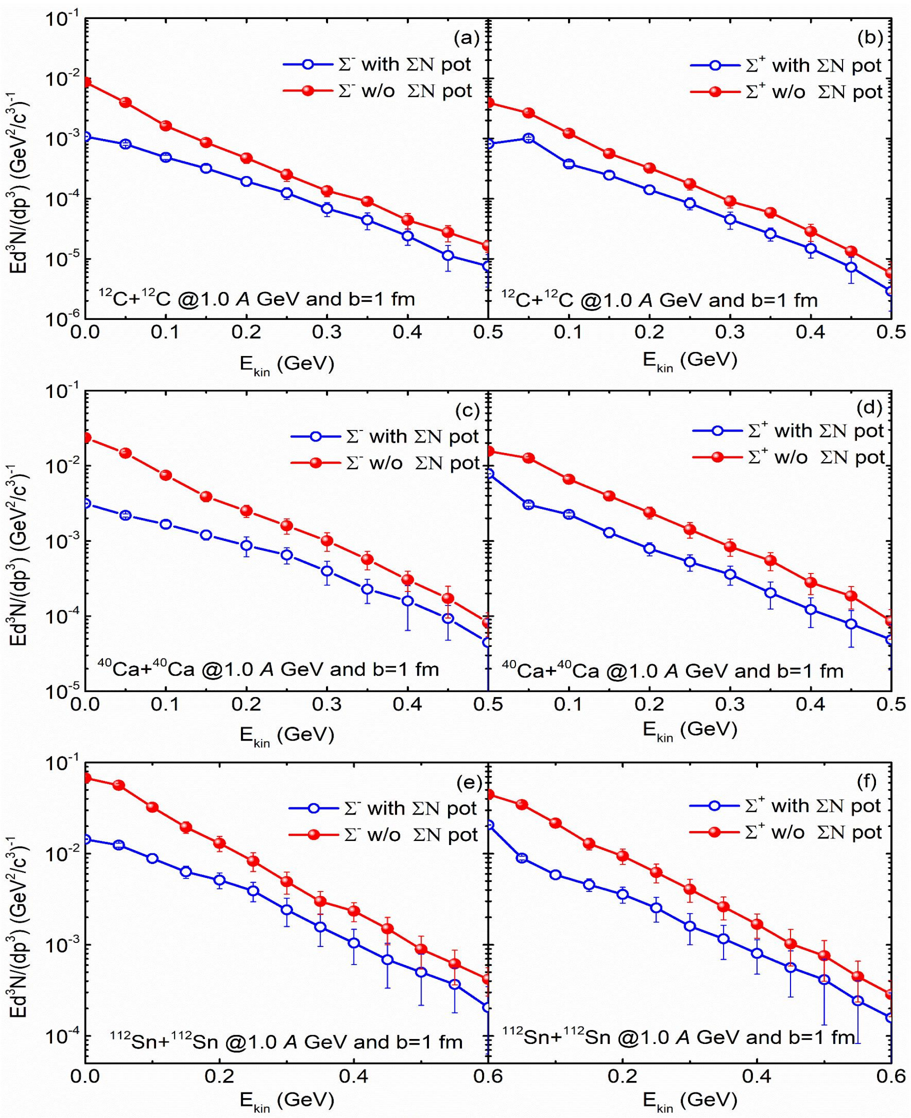

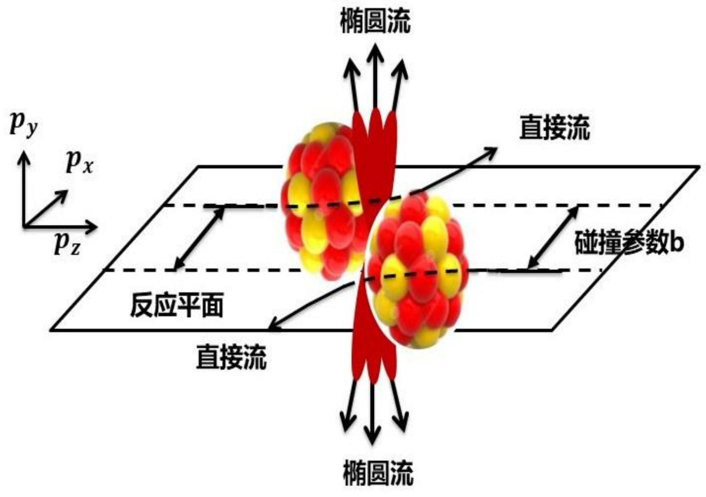

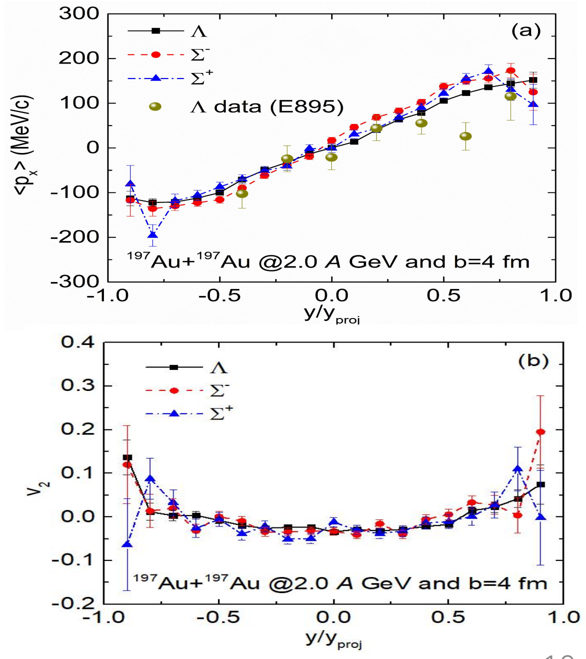

4. Hypernuclear production in HICs

H. Tamura, *Prog. Theor. Exp. Phys*. (2012) 02B012

① Neutron-rich/proton-rich HN nuclei and spectroscopies

② Multistrangeness HN (S=-2) $_{\Lambda\Lambda}X$和$_{\Xi}X$

③ Interaction potentials of NΛ, NΞ NNΛ, etc

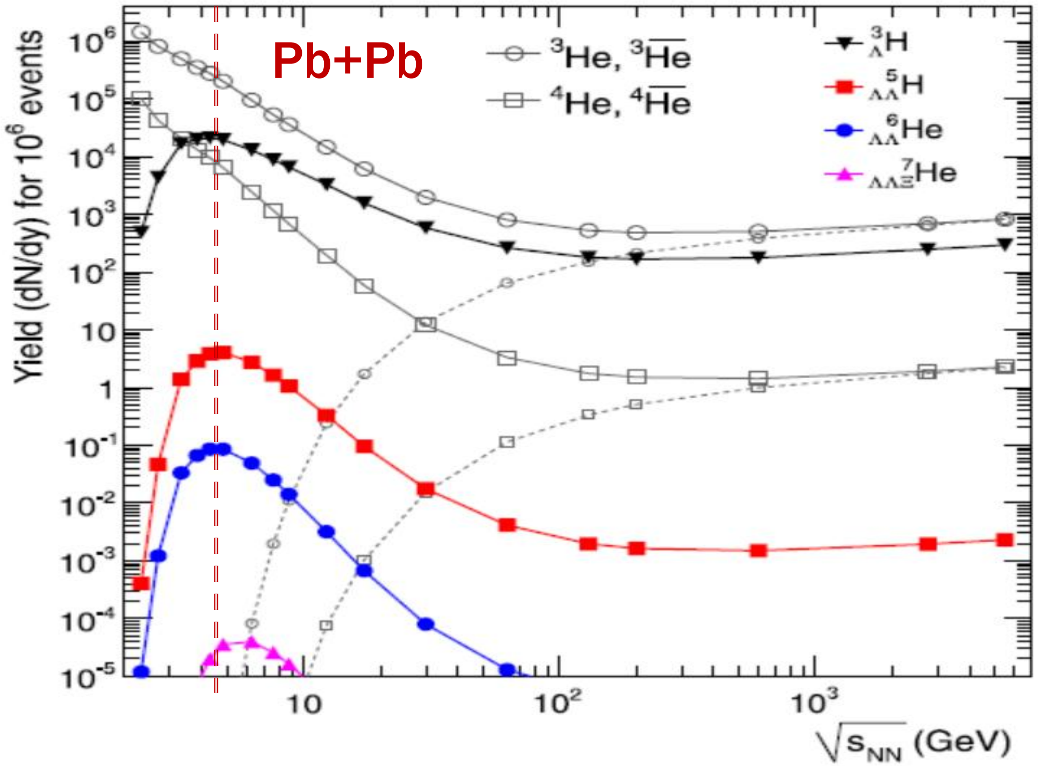

A. Andronic, P. Braun-Munzinger, J. Stachel, H. Stöcker, Physics Letters B 697 (2011) 203–207

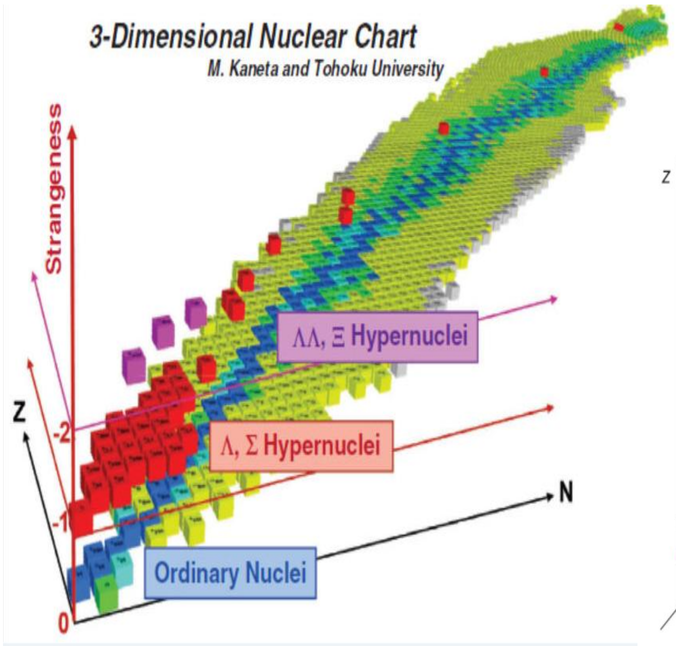

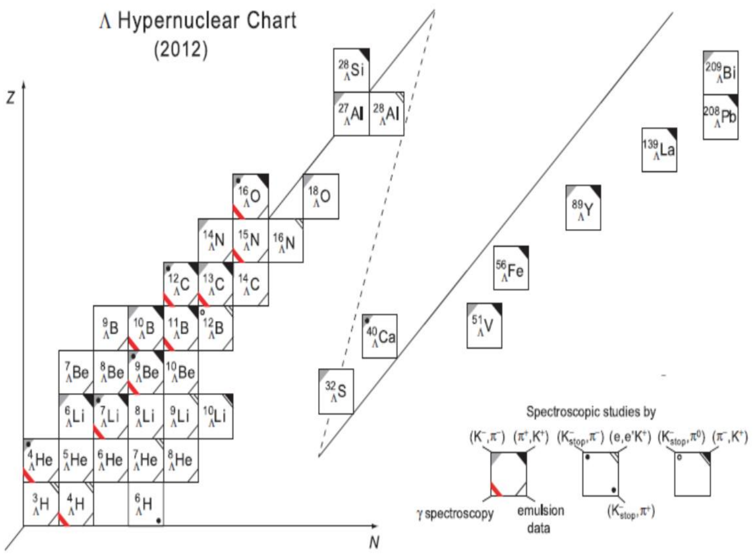

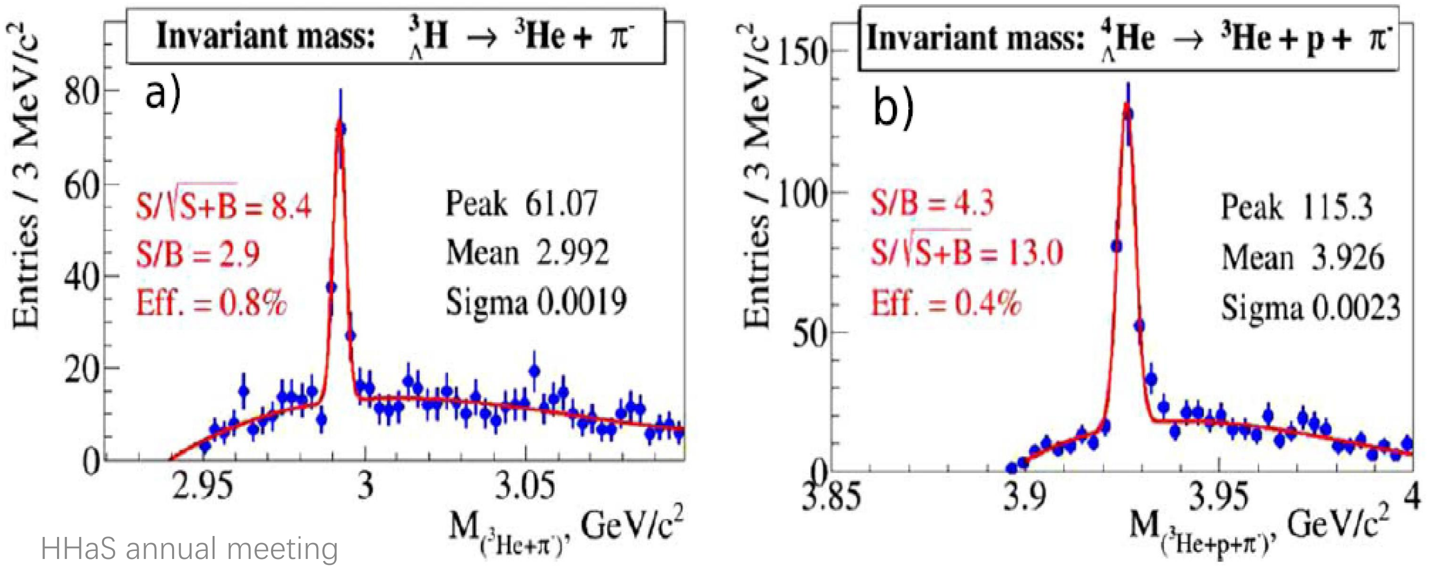

Transport model + coalescence approach

A.S. Botvina, J. Steinheimer, E.Bratkovskaya et al., Physics Letters B 742 (2015)7–14

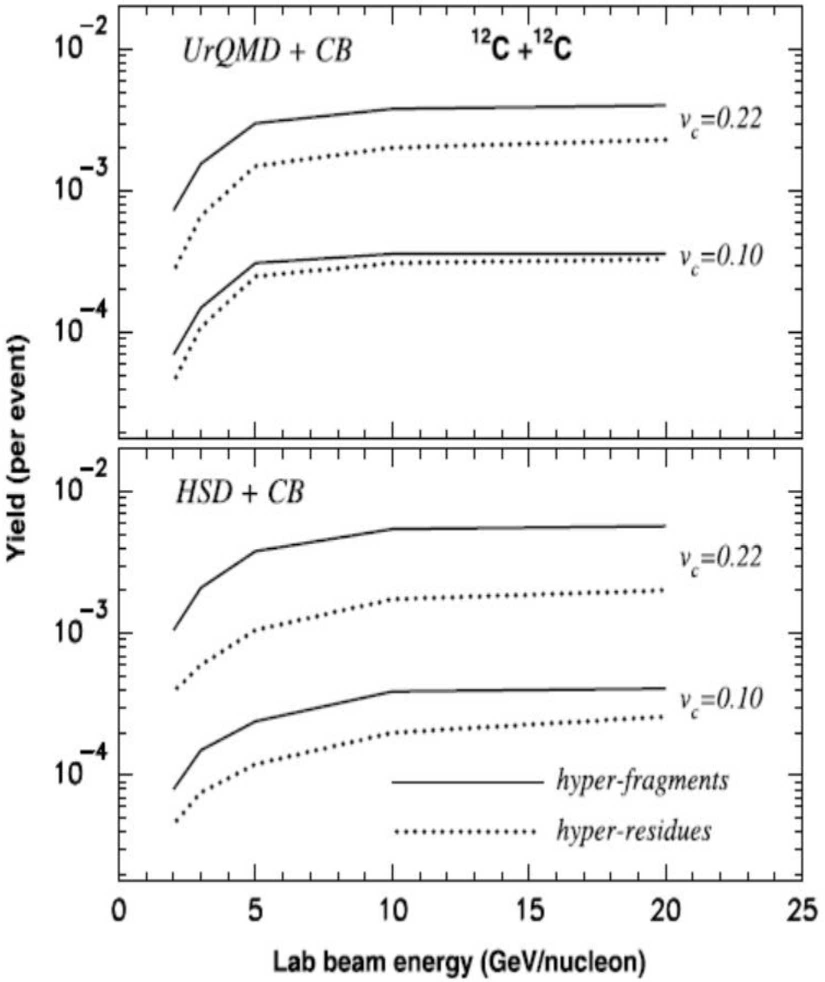

J. Aichelin, E. Bratkovskaya, A. Le Fèvre et al., Physical Review C 101, 044905 (2020)
A. Le Fèvre, J. Aichelin, C. Hartnack and Y. Leifels 100, Physical Review C 034904 (2019)

^{6}Li+^{12}C@2A GeV

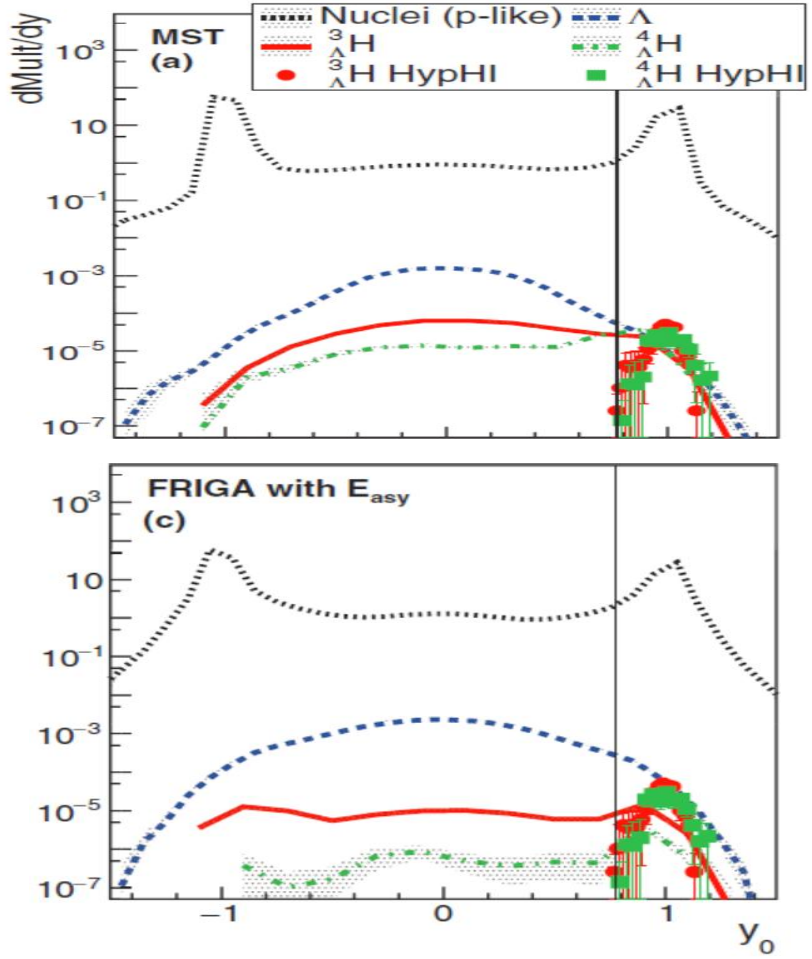

科学通报 2018 年 第 63 卷 第 8 期：735～744
论 文
《中国科学》杂志社 SCIENCE CHINA PRESS

中高能重离子碰撞中奇异粒子产生和超核形成机制

冯兆庆
中国科学院近代物理研究所, 兰州 730000
E-mail: fengzhq@impcas.ac.cn

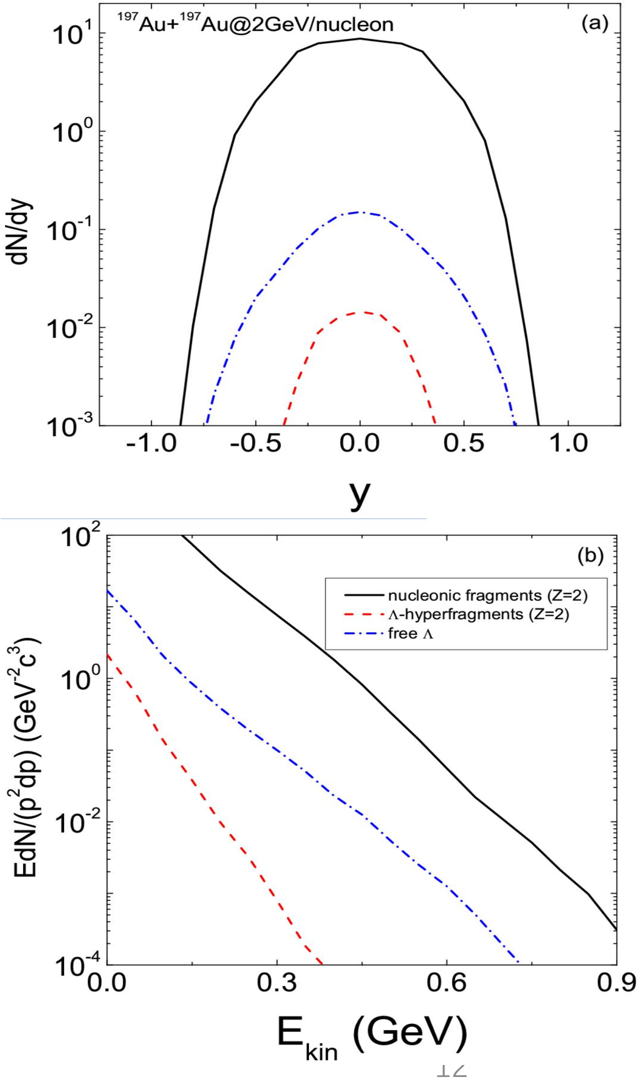

Hyperons in neutron stars (NS)

S. Weissenborn, D. Chatterjee, J. Schaffner-Bielich, Nucl. Phys. A 881, 62 (2012)

W. Z. Jiang, R. Y. Yang, and D. R. Zhang, Phys. Rev. C 87, 064314 (2013)

Diego Lonardoni, Alessandro Lovato, Stefano Gandolfi, and Francesco Pederiva, Phys. Rev. Lett. 114, 092301 (2015)

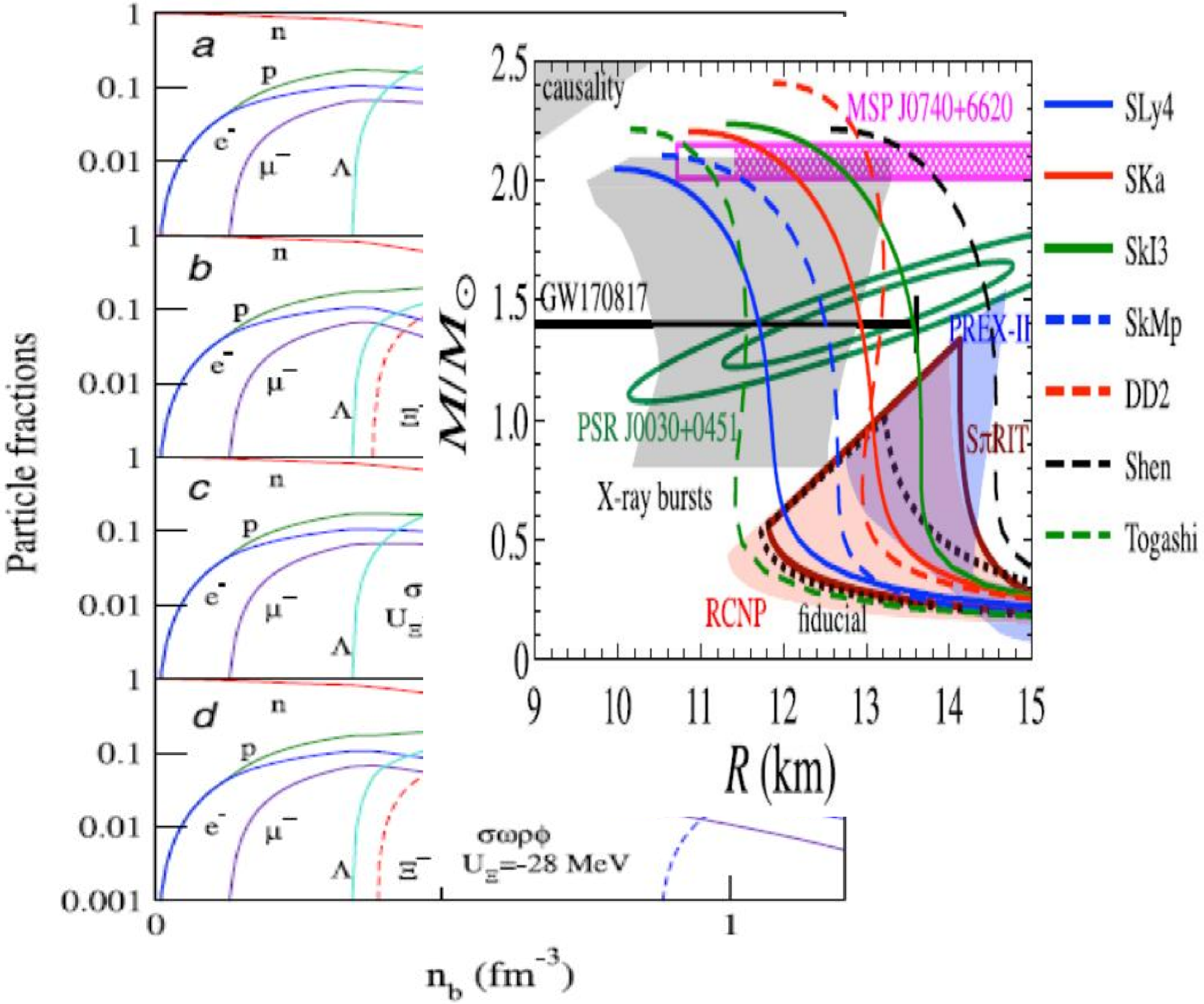

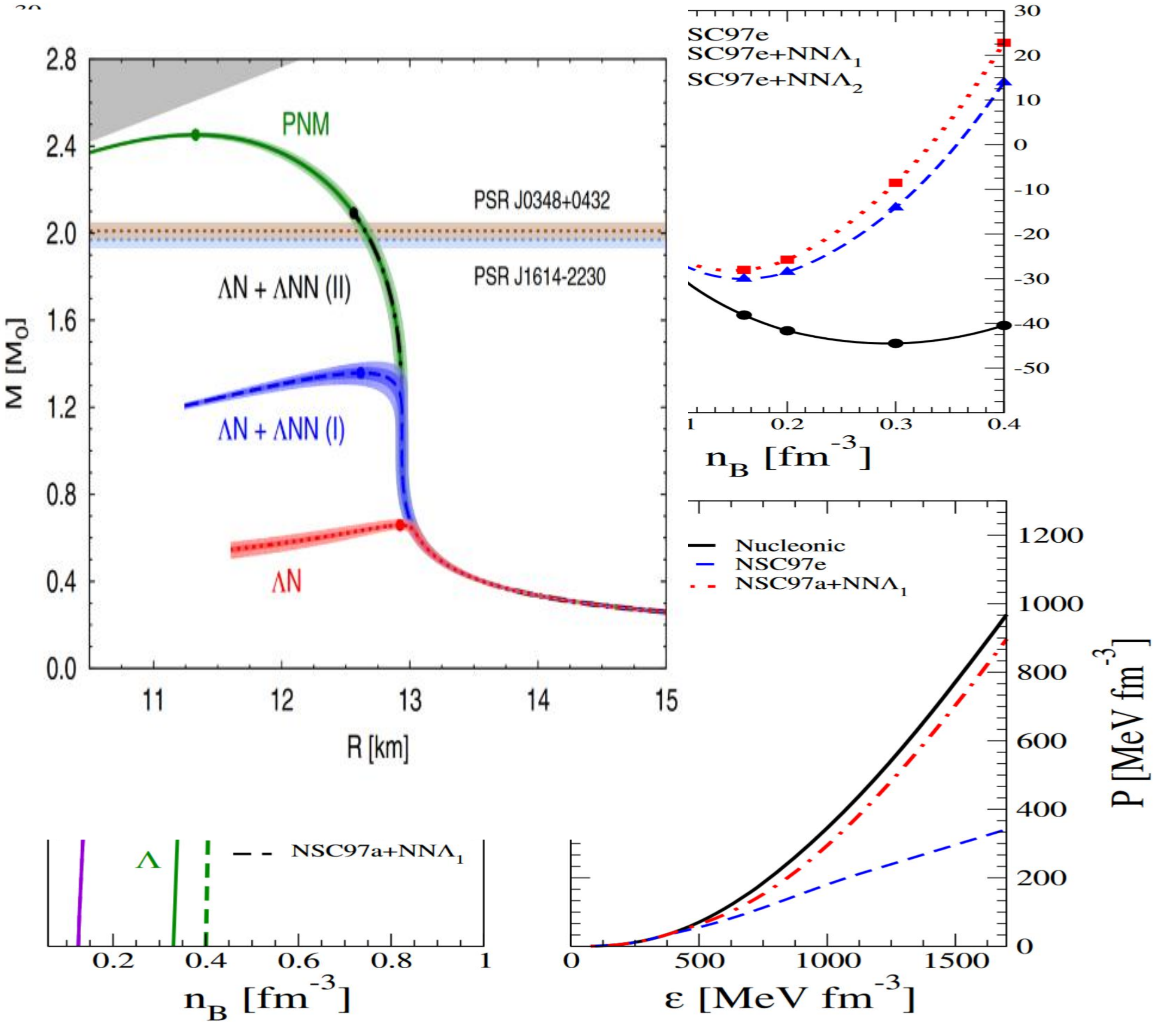

物 理 学 报 *Acta Phys. Sin.* **Vol. 74, No. 11 (2025) 112101**

《物理学报》创刊 90 周年

中高能重离子碰撞与核物质状态方程研究*

张亚鹏[1)2)] 孙志宇[1)2)†] 雍高产[1)2)] 冯兆庆[1)3)]

1) (中国科学院近代物理研究所, 重离子科学与技术全国重点实验室, 兰州 730000)

2) (中国科学院大学核科学与技术学院, 北京 100049)

3) (华南理工大学物理与光电学院, 广州 510641)

(2024 年 11 月 27 日收到; 2025 年 5 月 7 日收到修改稿)

核物质状态方程是对核物质体系在不同热力学或者外场条件下的宏观性质的描述, 它对理解微观强相互作用的理论——量子色动力学 (QCD)、原子核性质、重离子碰撞动力学、致密天体内部结构、双中子星合并等具有重要意义. 重离子碰撞 (HICs) 是在实验室产生极端条件 (如高温、高密、强磁场、强涡旋等) 核物质的唯一手段, 不同碰撞能量的 HICs 为定量研究核物质在不同热力学条件下的性质提供了可能. 本文主要介绍当前核物质状态方程的研究现状, 并介绍 HICs 中对核物质状态方程敏感的基本可观测量、探索核物质状态的典型实验和结果. 展现包含有奇异强子核物质状态方程的研究进展, 并探讨未来可能的研究方向. 介绍国际上在建和正在运行的重离子加速器和实验谱仪的最新进展, 包括我国已经建成的兰州重离子加速器装置 (HIRFL) 和兰州重离子加速器装置-冷却储存环 (HIRFL-CSR)、在建的强流重离子加速器装置 (HIAF) 和在建的低温高密核物质测量谱仪的研制进展, 并讨论未来基于我国大科学装置开展核物质状态方程实验研究的机遇与挑战.

关键词： 核物质状态方程, 重离子碰撞, 兰州重离子加速器装置-冷却储存环(HIRFL-CSR), 强流重离子加速器装置 (HIAF)

PACS： 21.65.Mn, 25.70.–z, 29.20.db **DOI:** 10.7498/aps.74.20241650

CSTR： 32037.14.aps.74.20241650

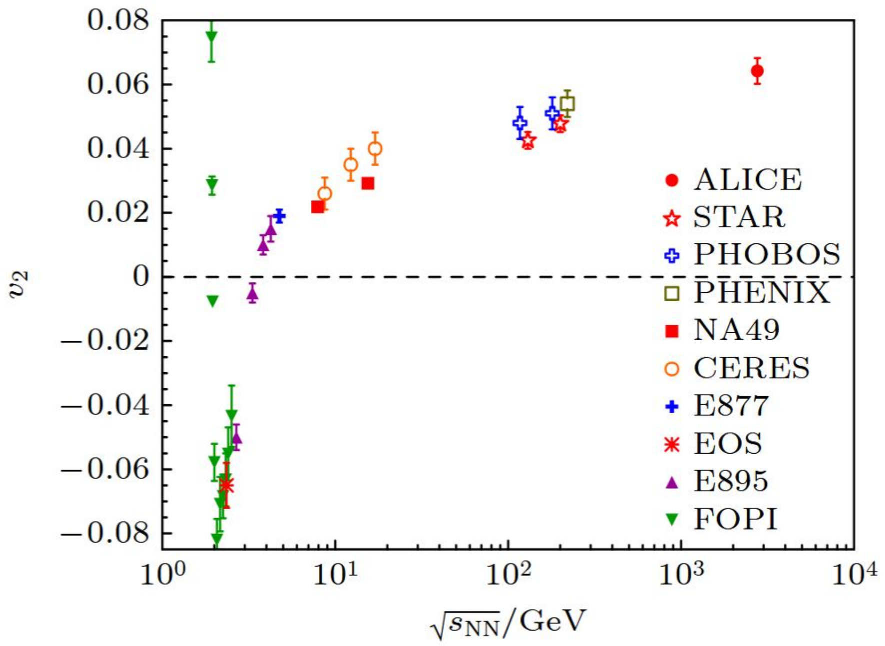

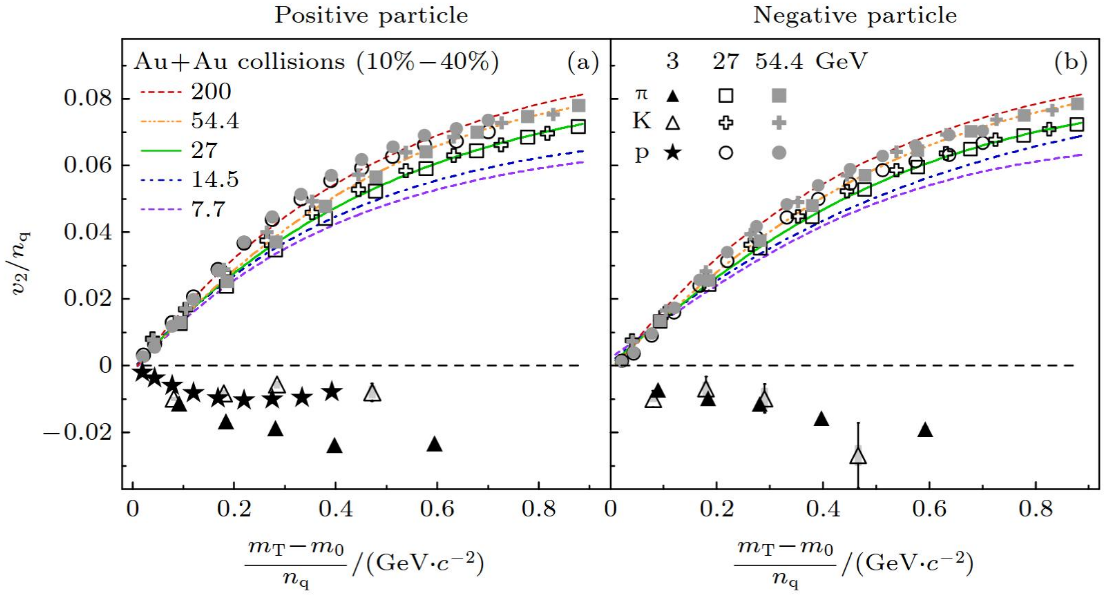

III. LQMD transport model

Lanzhou quantum molecular dynamics transport model (LQMD)

Heavy-ion collisions (5 MeV – 5 GeV/nucleon) and hadron induced reaction (p, $\bar{p}$, π, K, e, etc)

- **LQMD transport model** (Skyrme interaction, Walecka model with σ, ω, ρ, δ)
- **Neutron star equation of state via HICs** (nuclear symmetry energy at sub- and supra- saturation densities in HICs, isospin splitting of nucleon effective mass from HICs, particle production, 2-body and 3-body potential, multi-body correlation)
- **In-medium effects of hadrons** (optical potentials, energy conservation and in-medium effects, i.e., Δ(1232), N*(1440), N*(1535)), hyperons (Λ,Σ,Ξ) and mesons (π,K,η,ρ,ω,ϕ…))
- **Kinetic production of (hyper)clusters and nuclear fragmentation reactions** (production cross section, phase-space distribution, collective flows, cluster transportation, Mott effect, e.g., deuteron, triton, ^{3}He, α, $_{\Lambda(\Sigma)}X$, $_{\Lambda\Lambda}X$, $_{\Xi}X$, $_{\bar{\Lambda}}X$)
- **Nuclear collisions of light systems** (e.g., d+α, ^{9}Be+D_2O, d+^{7}Li etc, antisymmetrization with Volkov 2-body force)
- **Spallation reactions induced by p, d, t, α, $\bar{p}$, $\bar{d}$ etc (cascade multi-step collision for thick targets)**

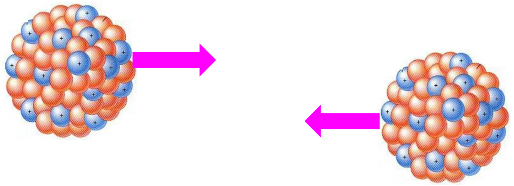

1. Lanzhou quantum molecular dynamics transport model (LQMD-Skyrme)

$$H_B = \sum_i \sqrt{\mathbf{p}_i^2 + \mathbf{m}_i^2} + U_{\text{int}} + U_{\text{mom}}$$

$$U_{loc} = \int V_{loc}(\rho(\mathbf{r}))\, d\mathbf{r}$$

PHYSICAL REVIEW C 84, 024610 (2011)

Momentum dependence of the symmetry potential and its influence on nuclear reactions

Zhao-Qing Feng*

Institute of Modern Physics, Chinese Academy of Sciences, Lanzhou 730000, People's Republic of China

(Received 11 July 2011; published 19 August 2011)

$$V_{loc}(\rho) = \frac{\alpha}{2}\frac{\rho^2}{\rho_0} + \frac{\beta}{1+\gamma}\frac{\rho^{1+\gamma}}{\rho_0^{\gamma}} + E_{sym}^{loc}(\rho)\rho\delta^2 + \frac{g_{sur}}{2\rho_0}(\nabla\rho)^2 + \frac{g_{sur}^{iso}}{2\rho_0}[\nabla(\rho_n - \rho_p)]^2,$$

Phys. Rev. C 84, 024610 (2011); 85, 014604 (2012)

$$U_{mom} = \frac{1}{2\rho_0}\sum_{i,j,j\neq i}\sum_{\tau,\tau'} C_{\tau,\tau'}\delta_{\tau,\tau_i}\delta_{\tau',\tau_j}\iiint d\mathbf{p}\,d\mathbf{p}'\,d\mathbf{r}\, f_i(\mathbf{r},\mathbf{p},t) \times[\ln(\epsilon(\mathbf{p}-\mathbf{p}')^2+1)]^2 f_j(\mathbf{r},\mathbf{p}',t).$$

C_{sym}= 38 MeV

a_{sym}= 37.7 MeV

b_{sym}= -18.7 MeV

$$E_{sym}(\rho) = \frac{1}{3}\frac{\hbar^2}{2m}\left(\frac{3}{2}\pi^2\rho\right)^{2/3} + E_{sym}^{loc}(\rho) + E_{sym}^{mom}(\rho).$$

$$E_{sym}^{loc}(\rho) = \frac{1}{2}C_{sym}(\rho/\rho_0)^{\gamma_s} \qquad E_{sym}^{loc}(\rho) = a_{sym}(\rho/\rho_0) + b_{sym}(\rho/\rho_0)^2.$$

Table 1: The parameters and properties of isospin symmetric EoS used in the LQMD model at the density of 0.16 fm^{-3}.

Parameters	α (MeV)	β (MeV)	γ	C_{mom} (MeV)	ϵ (c^2/MeV^2)	m^*_∞/m	K_∞ (MeV)
PAR1	-215.7	142.4	1.322	1.76	5×10^{-4}	0.75	230
PAR2	-226.5	173.7	1.309	0.	0.	1.	230

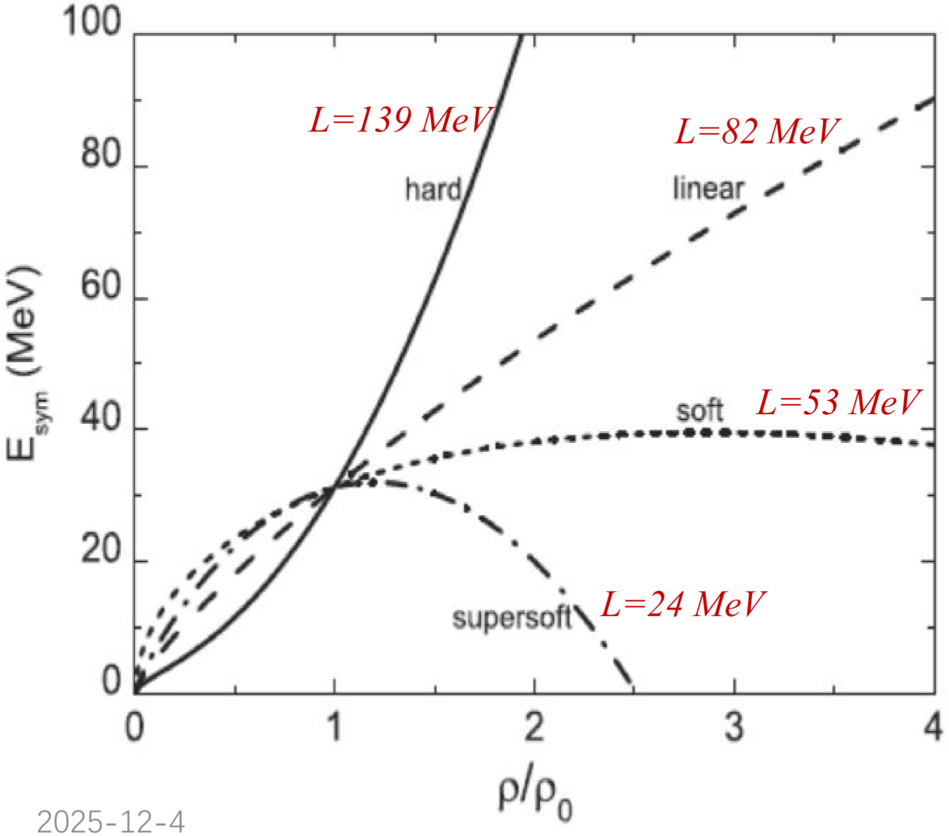

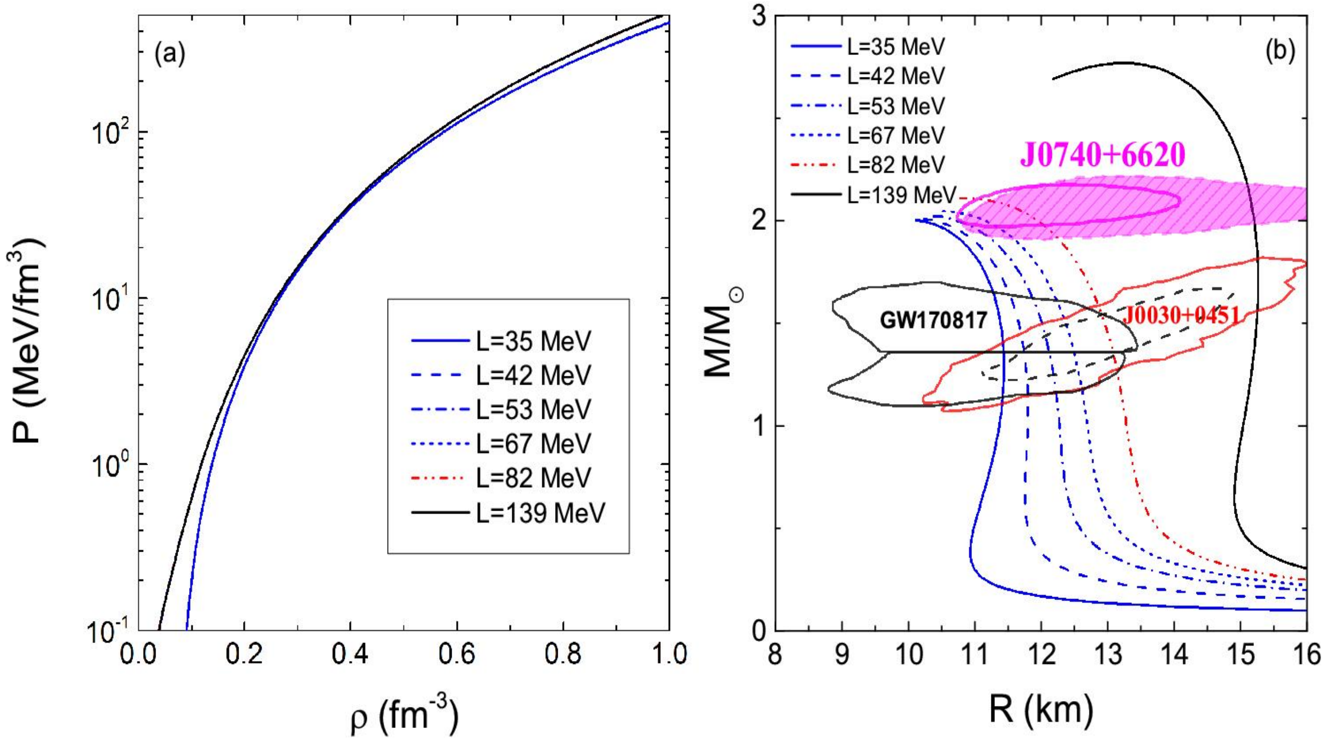

2. Covariant energy-density functional (LQMD.RMF)

Si-Na Wei, Zhao-Qing Feng, Nuclear Science and Techniques 35, 15 (2024) arXiv:2302.09984

$$
\begin{aligned}
L = {} & \bar{\psi}[i\gamma_\mu\partial^\mu - (M_N - g_\sigma\varphi - g_\delta\vec{\tau}\cdot\vec{\delta}) - g_\omega\gamma_\mu\omega^\mu - g_\rho\gamma_\mu\vec{\tau}\cdot\vec{b}^\mu]\psi \\
& + \frac{1}{2}(\partial_\mu\varphi\partial^\mu\varphi - m_\sigma^2\varphi^2) - U(\varphi) + \frac{1}{2}(\partial_\mu\vec{\delta}\partial^\mu\vec{\delta} - m_\sigma^2\vec{\delta}^2) \\
& + \frac{1}{2}m_\omega^2\omega_\mu\omega^\mu - \frac{1}{4}F_{\mu\nu}F^{\mu\nu} + \frac{1}{2}m_\rho^2\vec{b}_\mu\vec{b}^\mu - \frac{1}{4}\vec{G}_{\mu\nu}\vec{G}^{\mu\nu}
\end{aligned}
$$

$$
\begin{aligned}
F_{\mu\nu} &= \partial_\mu\omega_\nu - \partial_\nu\omega_\mu, \\
G_{\mu\nu} &= \partial_\mu\vec{b}_\nu - \partial_\nu\vec{b}_\mu, \\
U(\varphi) &= \frac{g_2}{3}\varphi^3 + \frac{g_3}{4}\varphi^4
\end{aligned}
$$

Energy density functional

$$
\varepsilon = \sum_{i=n,p} 2\int \frac{d^3k}{(2\pi)^3}\sqrt{k^2 + M_i^{*2}} + \frac{1}{2}m_\sigma^2\varphi^2 + U(\varphi) + \frac{1}{2}m_\omega^2\omega_0^2 + \frac{1}{2}m_\rho^2 b_0^2 + \frac{1}{2}m_\delta^2\delta_3^2
$$

Temporal evolution in phase space

$$
\begin{aligned}
\dot{\mathbf{x}} = {} & \frac{\mathbf{p_i^*}}{p_0^*} + \sum_{i\neq j}^{N}\{\frac{g_v^2}{2m_v^2}z_j^{*\mu}u_{i,\mu}B_iB_j\frac{\partial\rho_{ij}}{\partial\mathbf{p_i}} + \frac{g_v^2}{2m_v^2}z_i^{*\mu}u_{j,\mu}B_iB_j\frac{\partial\rho_{ji}}{\partial\mathbf{p_i}} + \frac{g_v^2}{2m_v^2}z_j^{*\mu}\rho_{ji}B_iB_j\frac{\partial u_{i,\mu}}{\partial\mathbf{p_i}} \\
& + z_j^{*\mu}\frac{B_iB_j\bar{g}_v^2}{2m_v^2}[\frac{\rho_{ij}}{1 - p_{T,ij}^2/\Lambda_v^2}\frac{\partial u_{i,\mu}}{\partial\mathbf{p_i}} + \frac{u_{i,\mu}}{1 - p_{T,ij}^2/\Lambda_v^2}\frac{\partial\rho_{ij}}{\partial\mathbf{p_i}} + u_{i,\mu}\rho_{ij}\frac{\partial[1/(1 - p_{T,ij}^2/\Lambda_v^2)]}{\partial\mathbf{p_i}}] \\
& + z_i^{*\mu}\frac{B_iB_j\bar{g}_v^2}{2m_v^2}[\frac{u_{j,\mu}}{1 - p_{T,ji}^2/\Lambda_v^2}\frac{\partial\rho_{ji}}{\partial\mathbf{p_i}} + u_{j,\mu}\rho_{ji}\frac{\partial[1/(1 - p_{T,ji}^2/\Lambda_v^2)]}{\partial\mathbf{p_i}}] \\
& - \frac{m_j^*}{p_j^{*0}}\frac{\partial S_j}{\partial\mathbf{p_i}} - \frac{m_i^*}{p_i^{*0}}\frac{\partial S_i}{\partial\mathbf{p_i}}\},
\end{aligned}
$$

$$
\begin{aligned}
\dot{\mathbf{p}} = {} & -\sum_{i\neq j}^{N}\{\frac{g_v^2}{2m_v^2}z_j^{*\mu}u_{i,\mu}B_iB_j\frac{\partial\rho_{ij}}{\partial\mathbf{r_i}} + \frac{g_v^2}{2m_v^2}z_i^{*\mu}u_{j,\mu}B_iB_j\frac{\partial\rho_{ji}}{\partial\mathbf{r_i}} \\
& + z_j^{*\mu}\frac{B_iB_j\bar{g}_v^2}{2m_v^2}\frac{u_{i,\mu}}{1 - p_{T,ij}^2/\Lambda_v^2}\frac{\partial\rho_{ij}}{\partial\mathbf{r_i}} \\
& + z_i^{*\mu}\frac{B_iB_j\bar{g}_v^2}{2m_v^2}\frac{u_{j,\mu}}{1 - p_{T,ji}^2/\Lambda_v^2}\frac{\partial\rho_{ji}}{\partial\mathbf{r_i}} \\
& - \frac{m_j^*}{p_j^{*0}}\frac{\partial S_j}{\partial\mathbf{r_i}} - \frac{m_i^*}{p_i^{*0}}\frac{\partial S_i}{\partial\mathbf{r_i}}\},
\end{aligned}
$$

TABLE I: Parameter sets for RMF. The saturation density ρ_0 is set to be 0.16 fm^{-3}. The binding energy of saturation density is $E/A - M_N = -16$ MeV. The isoscalar-vector ω and isovector-vector ρ masses are fixed to their physical values, $m_\omega = 783$ MeV and $m_\rho = 763$ MeV. The remaining meson mass m_σ is set to be 550 MeV.

model	g_σ	g_ω	g_2 (fm^{-1})	g_3	g_ρ	g_δ	K (MeV)	$E_{sym}(\rho_0)$ (MeV)	L (ρ_0)(MeV)
set1	8.145	7.570	31.820	28.100	4.049	-	230	31.6	85.3
set2	8.145	7.570	31.820	28.100	8.673	5.347	230	31.6	109.3
set3	8.145	7.570	31.820	28.100	11.768	7.752	230	31.6	145.0

Symmetry energy

$$E_{sym} = \frac{1}{6}\frac{k_F^2}{E_F^*} + \frac{1}{2}\left[f_\rho - f_\delta\left(\frac{M^*}{E_F^*}\right)\right]\rho$$

$$f_{\rho,\delta} = g_{\rho,\delta}/m_{\rho,\delta}$$

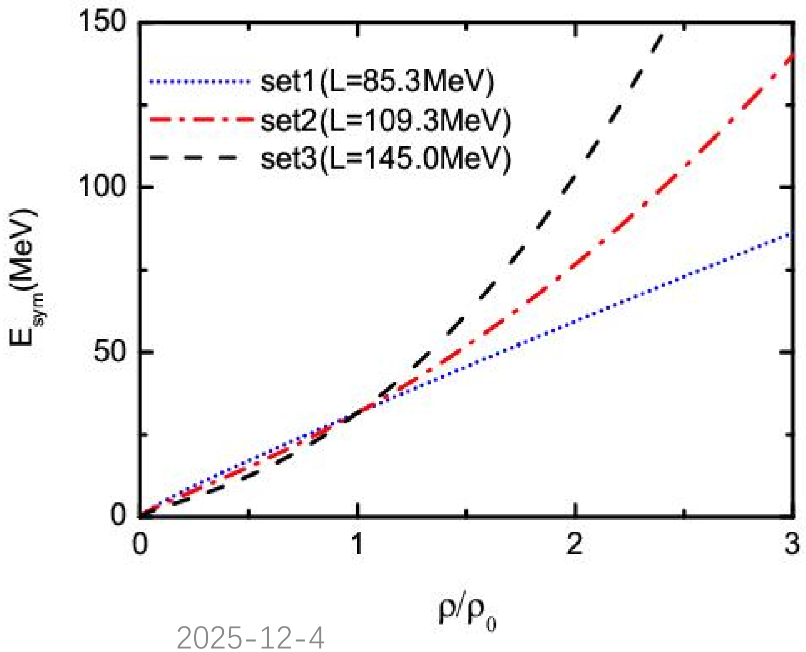

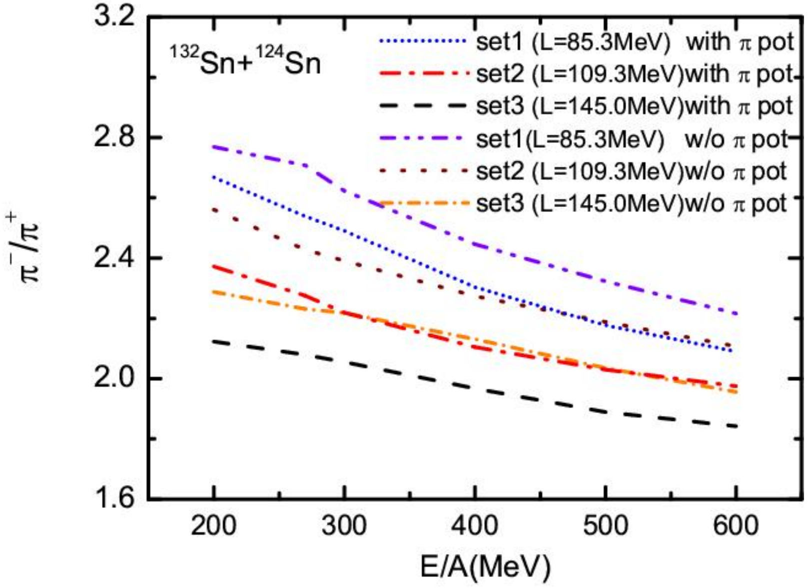

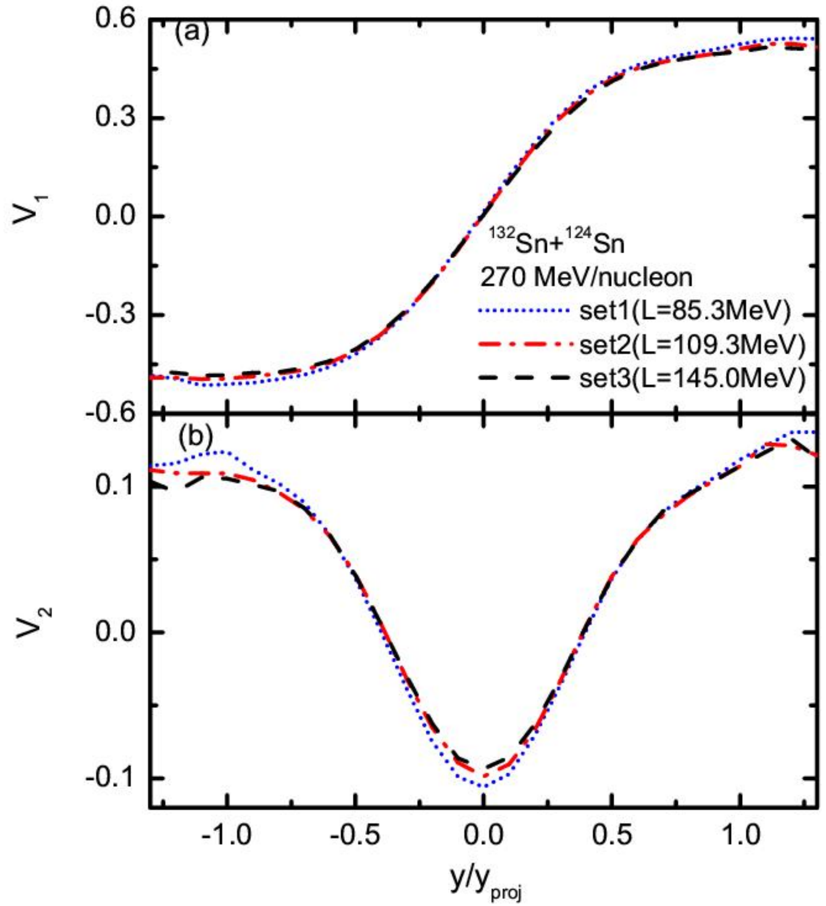

3. Particle production

π and resonances (Δ(1232), N*(1440), N*(1535), ...) production:

$$NN \leftrightarrow N\Delta, \quad NN \leftrightarrow NN^*, \quad NN \leftrightarrow \Delta\Delta, \quad \Delta \leftrightarrow N\pi,$$

$$N^* \leftrightarrow N\pi, \quad NN \leftrightarrow NN\pi(s-state), \quad N^*(1535) \leftrightarrow N\eta$$

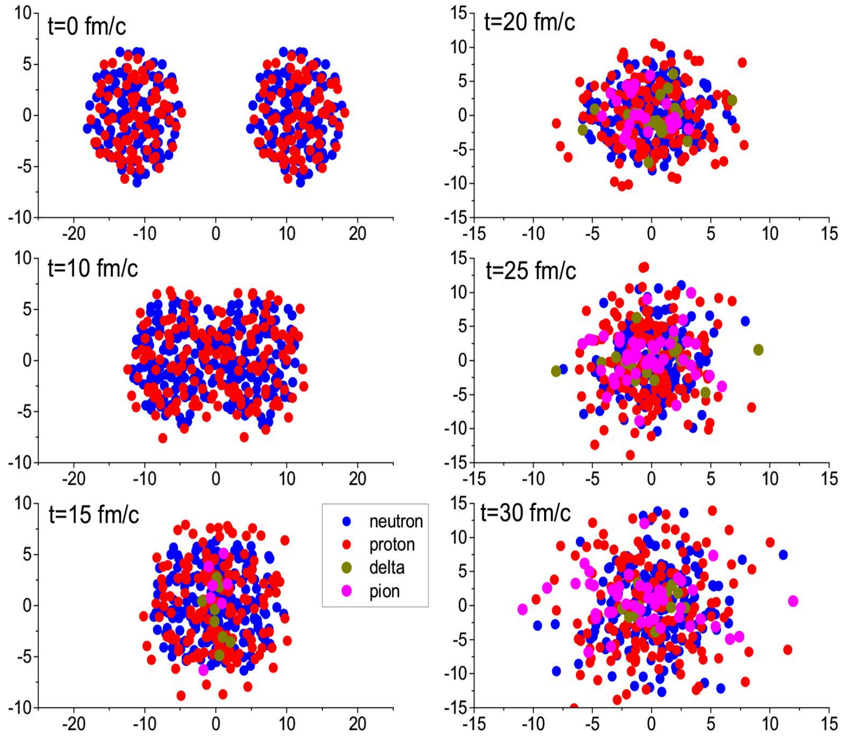

Collisions between resonances, NN*↔NΔ, NN*↔NN*

Strangeness channels:

$$BB \to BYK, BB \to BBK\overline{K}, B\pi(\eta) \to YK, YK \to B\pi,$$

$$B\pi \to NK\overline{K}, Y\pi \to B\overline{K}, \quad B\overline{K} \to Y\pi, \quad YN \to \overline{K}NN,$$

$$BB \to B\Xi KK, \overline{K}B \leftrightarrow K\Xi, YY \leftrightarrow N\Xi, \overline{K}Y \leftrightarrow \pi\Xi.$$

Reaction channels with antiproton:

$$\overline{p}N \to NN, \quad \overline{N}N \to \overline{N}N, \overline{N}N \to \overline{B}B, \overline{N}N \to \overline{Y}Y$$

$$\overline{N}N \to \text{annihilation}(\pi, \eta, \rho, \omega, K, \overline{K}, K^*, \overline{K}^*, \phi)$$

Statistical model with SU(3) symmetry for annihilation
(E.S. Golubeva et al., Nucl. Phys. A 537, 393 (1992))

The **PYTHIA** and **FRITIOF** code are used for baryon(meson)-baryon and antibaryon-baryon collisions at high invariant energies

4. Results I: Hyperon-nucleon interaction in dense nuclear matter via HICs

$$H_Y = \sum_{i=1}^{N_Y} V_i^{Coul} + V_{opt}^Y(\boldsymbol{p}_i, \rho_i) + \sqrt{\boldsymbol{p}_i^2 + m_Y^2}$$

$$V_{opt}^Y(\boldsymbol{p}_i, \rho_i) = \omega_Y(\boldsymbol{p}_i, \rho_i) - \sqrt{\boldsymbol{p}_i^2 + m_Y^2}$$

$$\omega_Y(\boldsymbol{p}_i, \rho_i) = \sqrt{(m_Y + \Sigma_S^Y)^2 + \mathbf{p}_i^2} + \Sigma_V^Y,$$

Phenomenological potential by fitting the results of chiral effective field theory

$$V_{opt}^{\Lambda}(\boldsymbol{p}_i, \rho_i) = V_a(\rho_i/\rho_0) + V_b(\rho_i/\rho_0)^2 + C_{mom}(\rho_i/\rho_0)\ln(\epsilon \boldsymbol{p}_i^2 + 1)$$

$$V_{opt}^{\Sigma}(\boldsymbol{p}_i, \rho_i) = V_0(\rho_i/\rho_0)^{\gamma_s} + V_1(\rho_n - \rho_p)t_{\Sigma}\rho_i^{\gamma_s -} + C_{mom}(\rho_i/\rho_0)\ln(\epsilon \boldsymbol{p}_i^2 + 1).$$

Phys. Lett. B 851 (2024) 138580

Contents lists available at ScienceDirect

Physics Letters B

journal homepage: www.elsevier.com/locate/physletb

ELSEVIER

Letter

Extracting the hyperon-nucleon interaction via collective flows in heavy-ion collisions

Zhao-Qing Feng

School of Physics and Optoelectronics, South China University of Technology, Guangzhou 510640, China

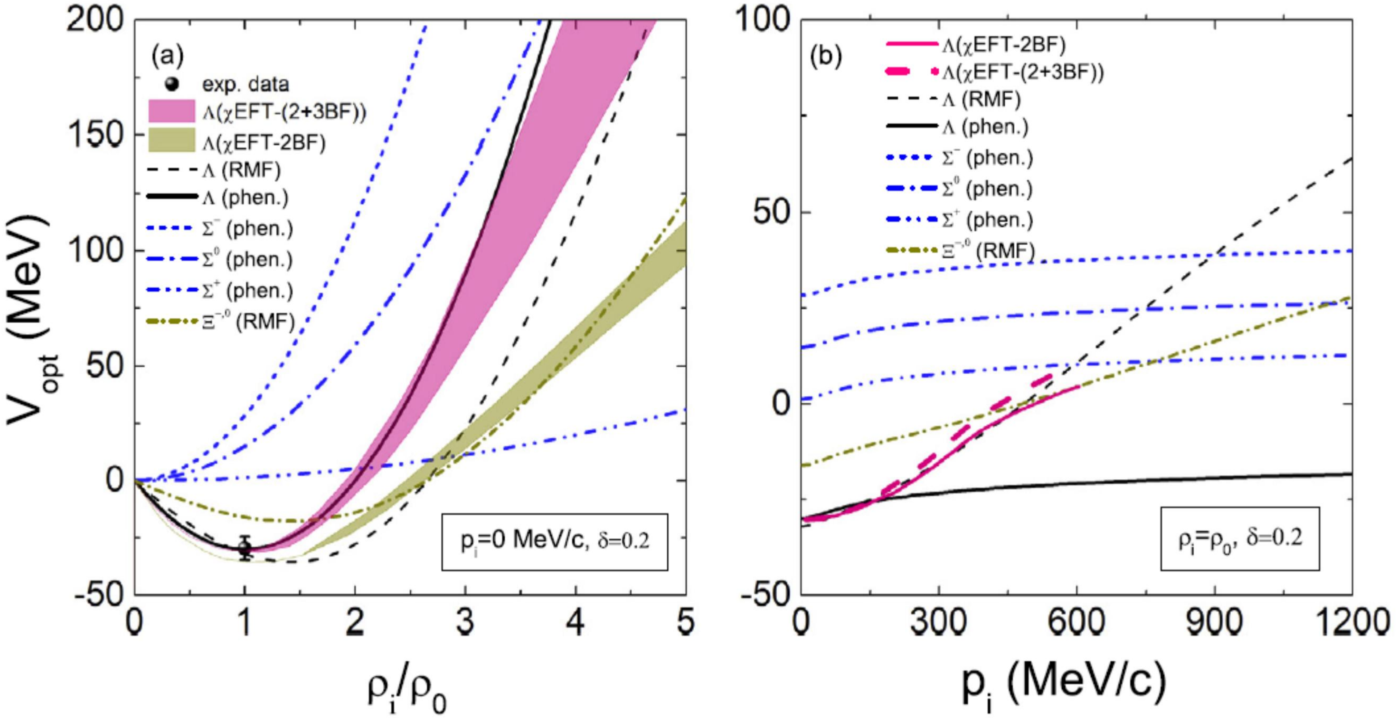

Hyperon-nucleon interaction in dense matter:

Extracting the hyperon-nucleon interaction via collective flows in heavy-ion collisions

Phys. Lett. B 851 (2024) 138580

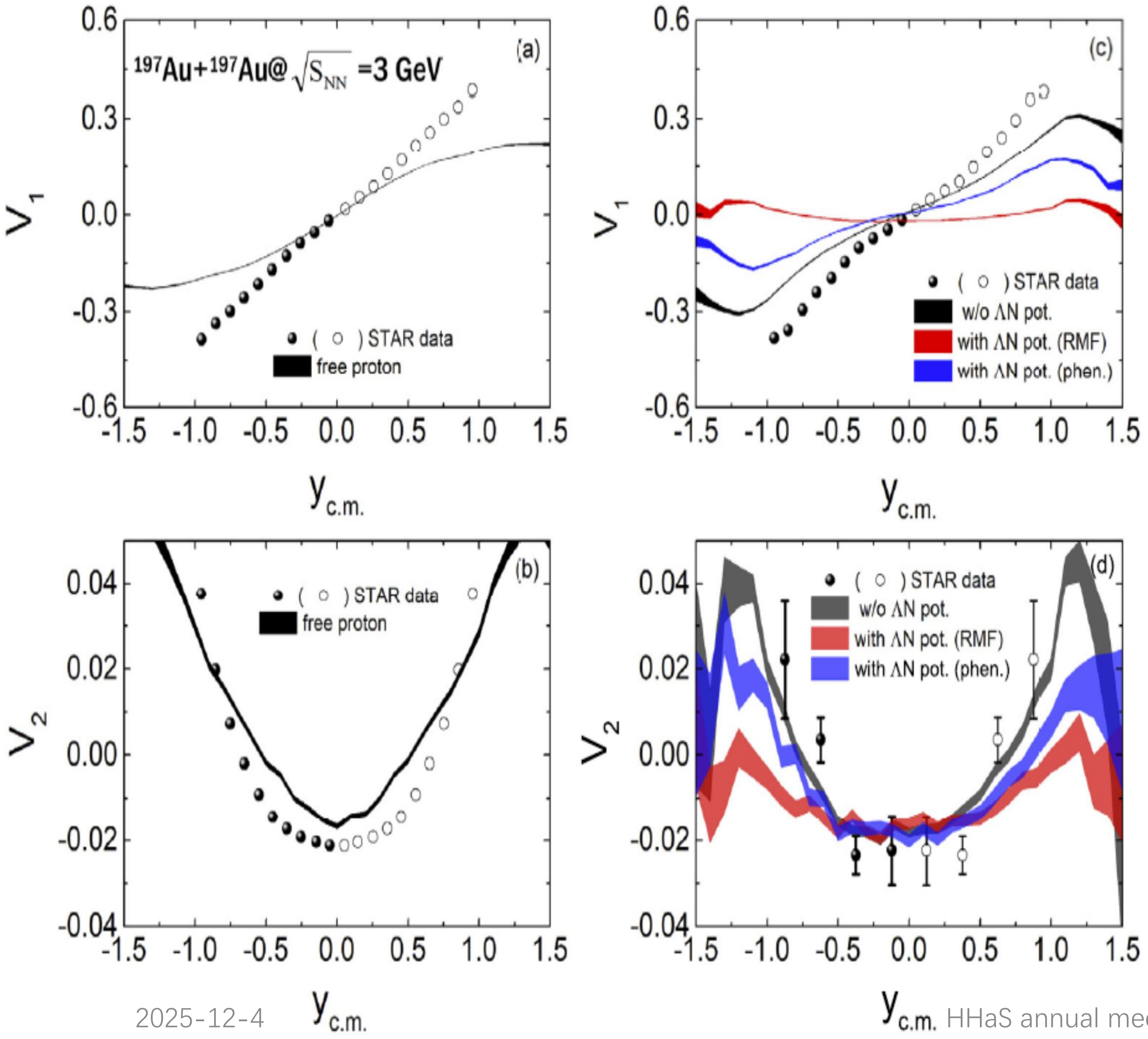

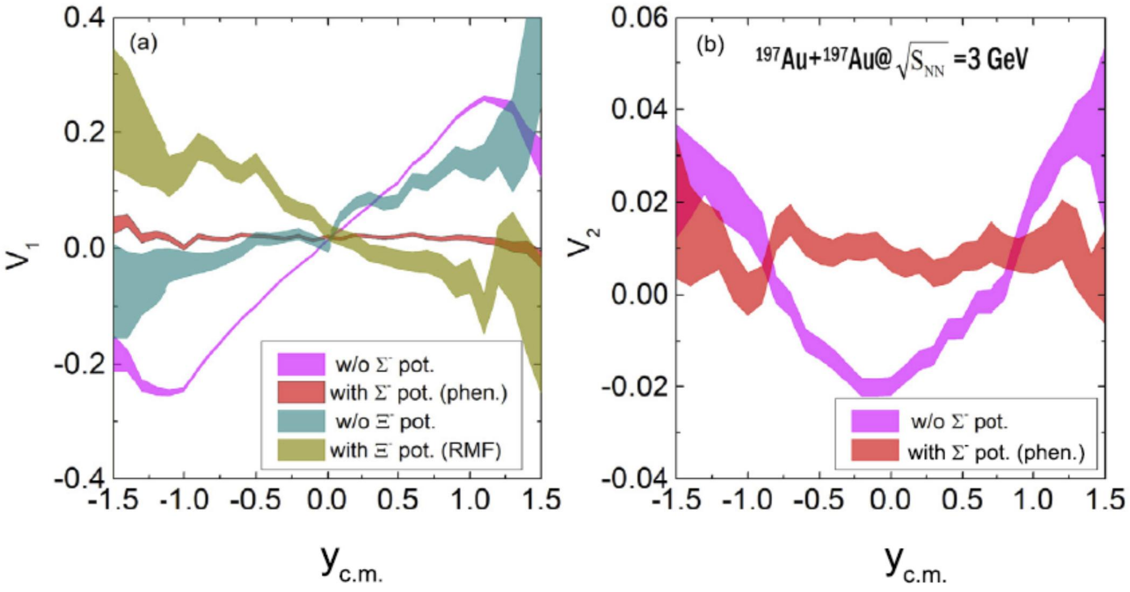

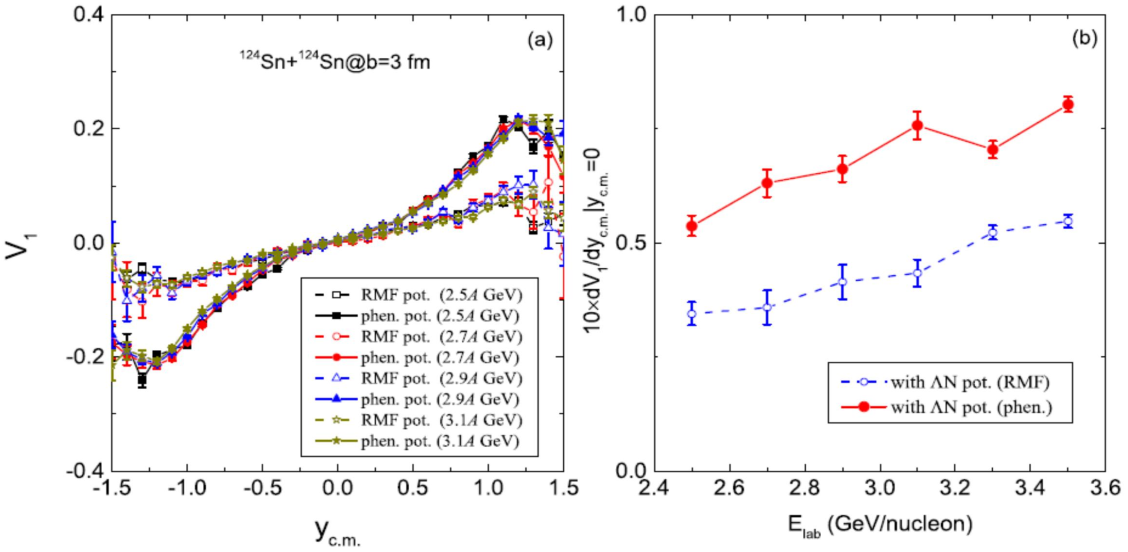

Hyperon-nucleon interaction in dense matter:

The general flavor SU(3) symmetry for hyperon-nucleon potential

$$\mathcal{L}_{int} = \sum_B \bar{\psi}_B [g_{B\sigma}\sigma - \gamma_\mu (g_{B\omega}\omega^\mu + g_{B\phi}\phi^\mu + g_{B\rho}\vec{\tau}\cdot\vec{b}^\mu)$$

$$]\psi_B - \frac{1}{3}g_2\sigma^3 - \frac{1}{4}g_3\sigma^4,$$

$$\frac{g_{\Lambda\omega}}{g_{N\omega}} = \frac{g_{\Sigma\omega}}{g_{N\omega}} = \frac{\sqrt{2}}{\sqrt{2}+\sqrt{3}z},$$

$$\frac{g_{\Lambda\phi}}{g_{N\omega}} = \frac{g_{\Sigma\phi}}{g_{N\omega}} = \frac{-1}{\sqrt{2}+\sqrt{3}z},$$

$$\frac{g_{\Xi\omega}}{g_{N\omega}} = \frac{\sqrt{2}-\sqrt{3}z}{\sqrt{2}+\sqrt{3}z},$$

$$\frac{g_{\Xi\phi}}{g_{N\omega}} = -\frac{1+\sqrt{6}z}{\sqrt{2}+\sqrt{3}z},$$

$$\frac{g_{N\phi}}{g_{N\omega}} = -\frac{\sqrt{6}z-1}{\sqrt{2}+\sqrt{3}z}.$$

Phys. Lett. B 853 (2024) 138658

Contents lists available at ScienceDirect

Physics Letters B

journal homepage: www.elsevier.com/locate/physletb

ELSEVIER

Letter

Correlation of the hyperon potential stiffness with hyperon constituents in neutron stars and heavy-ion collisions

Si-Na Wei [a], Zhao-Qing Feng [b,*], Wei-Zhou Jiang [c]

[a] School of Mathematics and Physics, Guangxi Minzu University, Nanning 530006, China

[b] School of Physics and Optoelectronics, South China University of Technology, Guangzhou 510640, China

[c] School of Physics, Southeast University, Nanjing 211189, China

LQMD.RMF

Phys. Lett. B 853 (2024) 138658

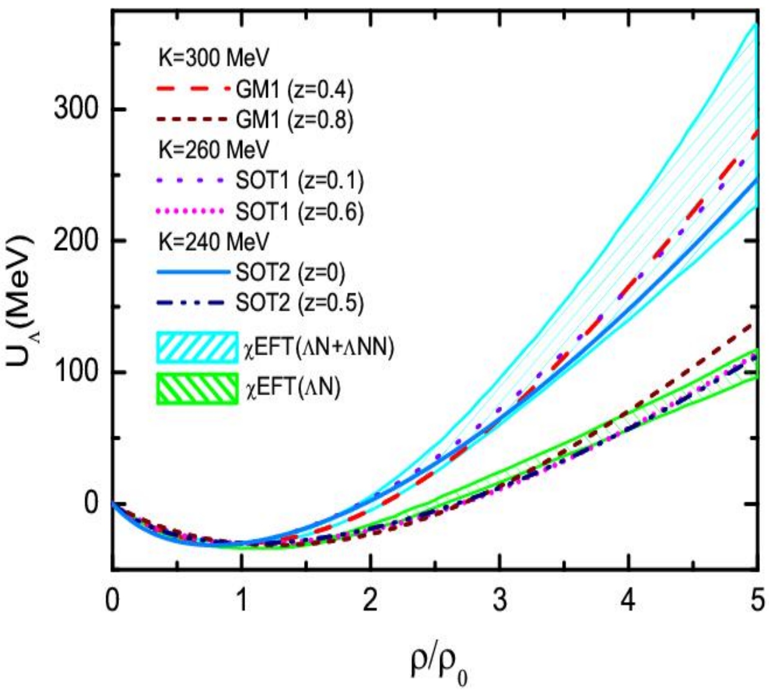

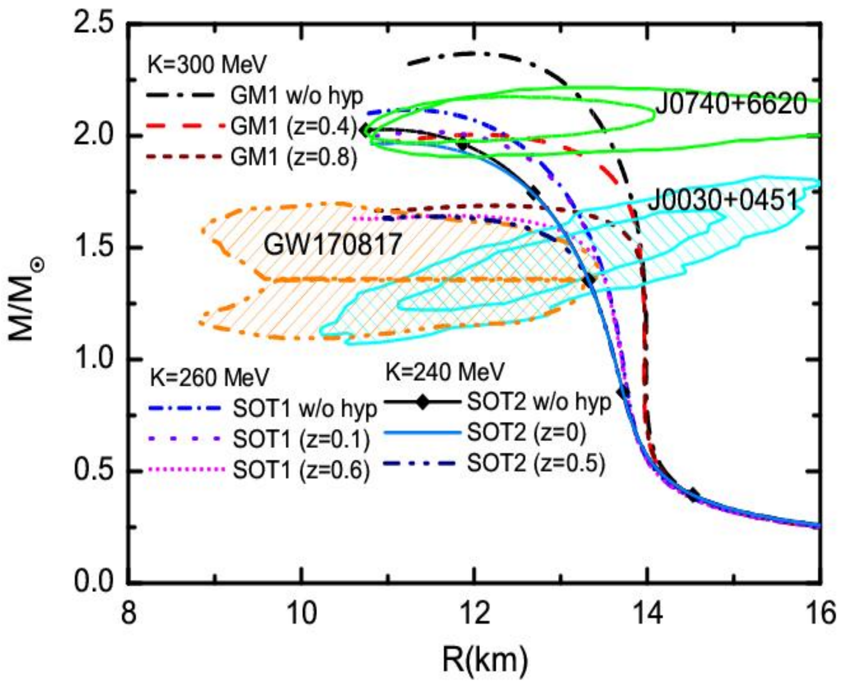

$$U_\Lambda(\rho_0) = -U_\Sigma(\rho_0) = -30\ \text{MeV}, U_\Xi(\rho_0) = -14\ \text{MeV}$$

Correlation of the hyperon potential stiffness with hyperon constituents in neutron stars and heavy-ion collisions

Si-Na Wei, ZQF, Wei-Zhou Jiang, PLB 853 (2024) 138658

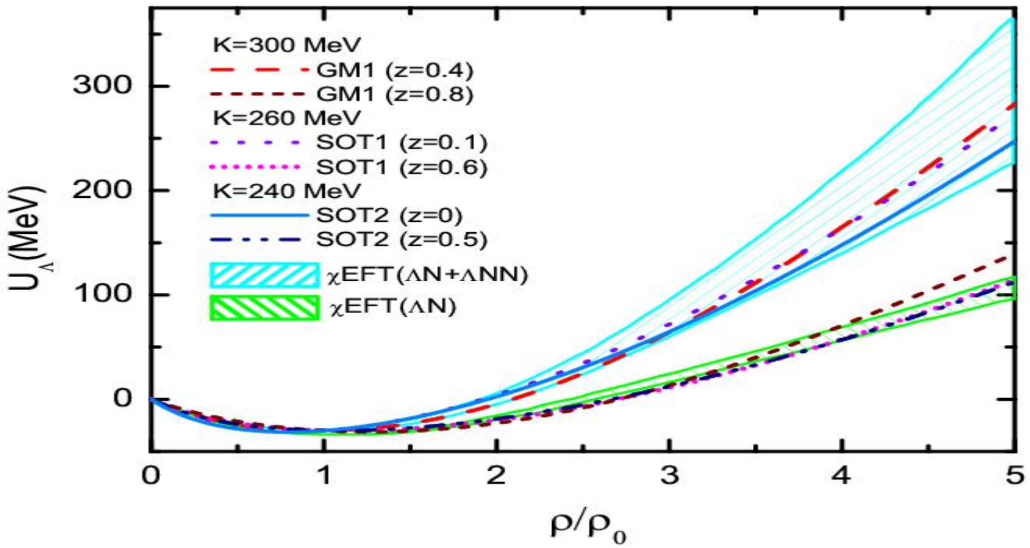

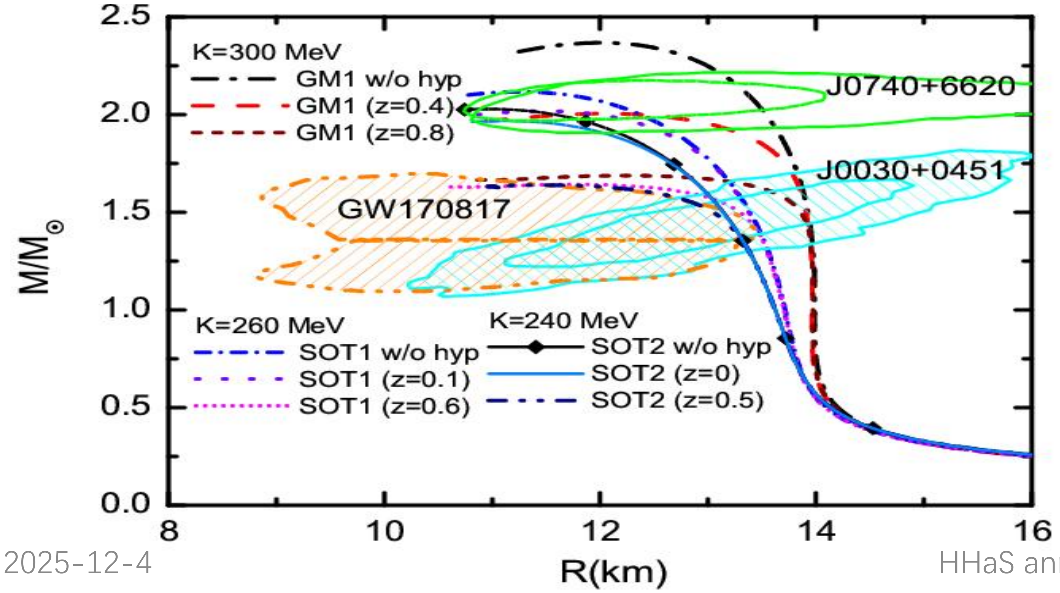

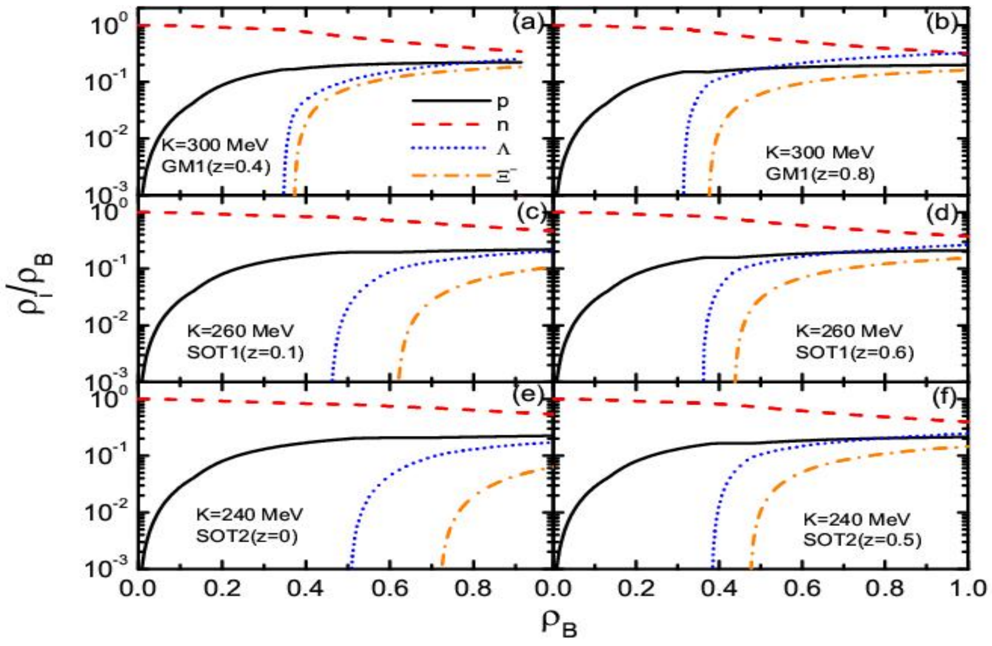

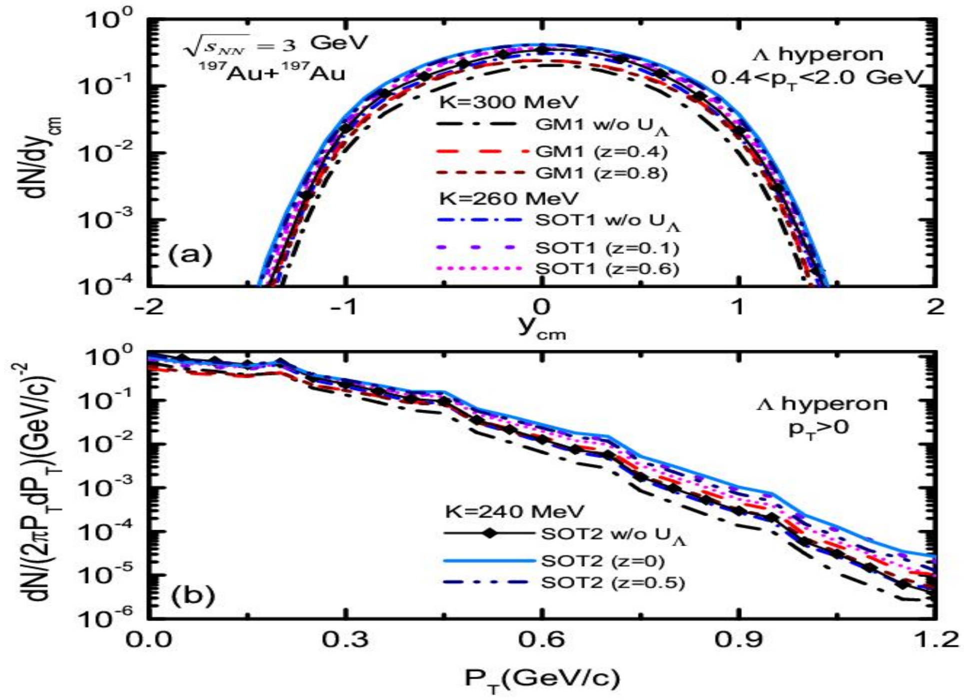

High-density symmetry energy from hyperon production in heavy-ion collisions, Physics Letters B 846 (2023) 138180

Contents lists available at ScienceDirect

Physics Letters B

journal homepage: www.elsevier.com/locate/physletb

Probing the high-density symmetry energy from subthreshold hyperon production in heavy-ion collisions

Zhao-Qing Feng

School of Physics and Optoelectronics, South China University of Technology, Guangzhou 510640, China

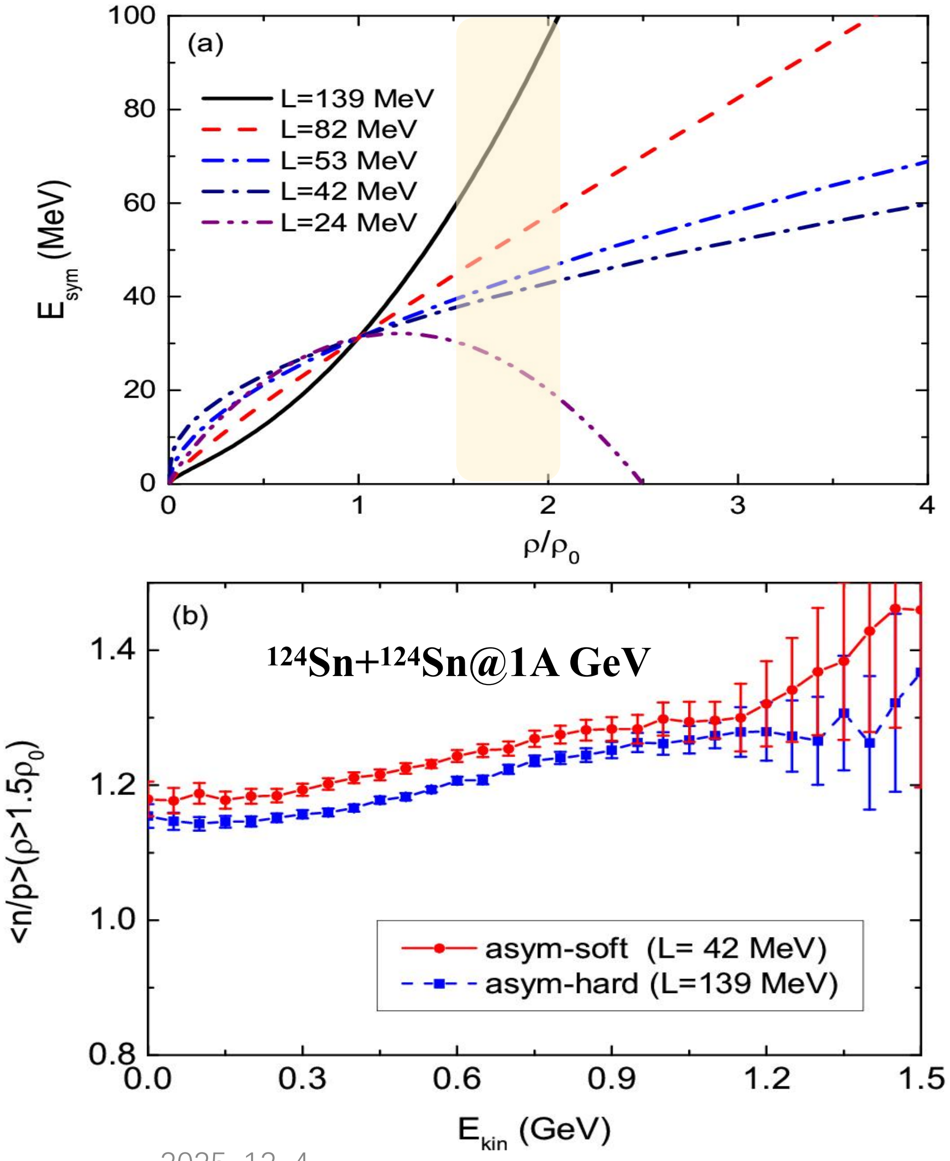

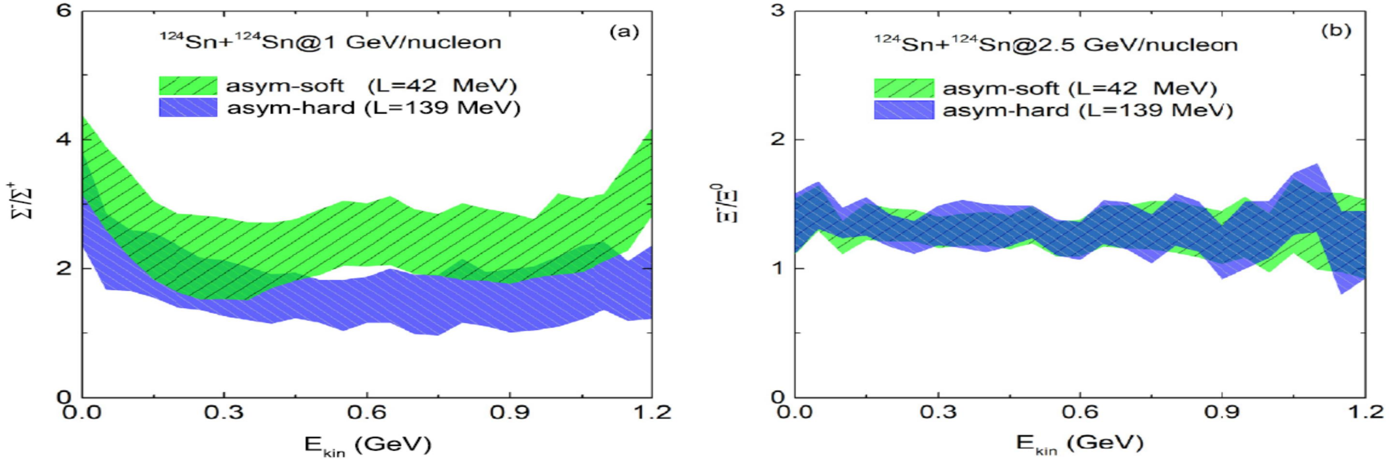

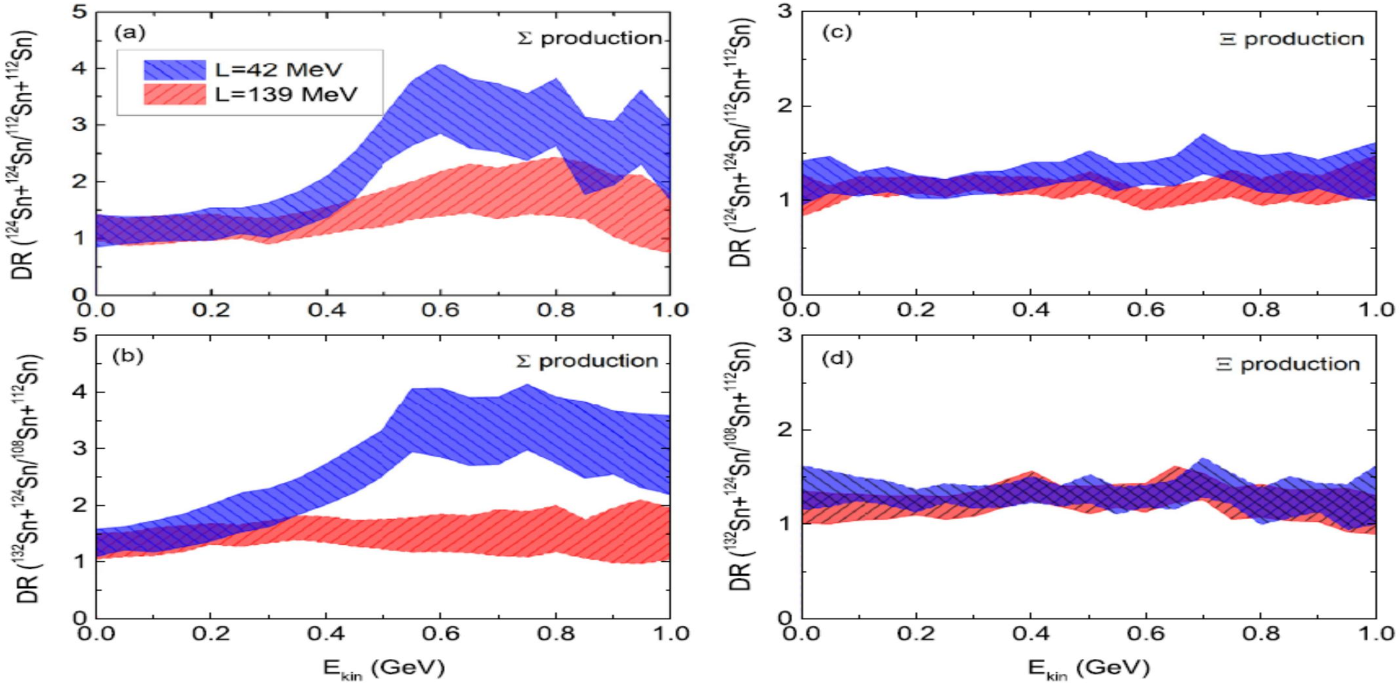

4. Results II: Fragmentation reaction and hyperfragment production in HICs

Kinetic approach (动理学) for cluster production

P. Danielewicz, G. F. Bertsch, Nuclear Physics A 533 (1991) 712-748
Akira Ono, Prog. Part. Nucl. Phys. 105, 139-179 (2019)
R. Wang, Y. G. Ma, L. W. Chen et al., Phys. Rev. C 108, L031601 (2023)
Hui-Gan Cheng, Zhao-Qing Feng, Phys. Rev. C 109, L021602 (2024)

Year	models	Author(s)	Cluster(s)	Energy	Treatment(s)
1991	**pBUU**	P. Danielewicz et al.	d, t, h	fermi /intermediate energies	kinetic, Mott cut
2013	**AMD-cluster**	A. Ono	$2N,\ 3N, \alpha$	fermi /intermediate energies	kinetic, fermionic mean field
2021	**SMASH**	J. Staudenmaier et al.	d	GeV and higher	kinetic
2022	**PHQMD**	G. Coci et al.	d	GeV and higher	kinetic
2023	**LBUU**	R. Wang et al.	$d,\ t,\ h, \alpha$	intermediate energies	kinetic, Mott cut
2023	**LQMD**	H. G. Cheng and Z. Q. Feng	$d,\ t,\ h, \alpha$	fermi /intermediate energies	Kinetic, binding energy, Pauli effects

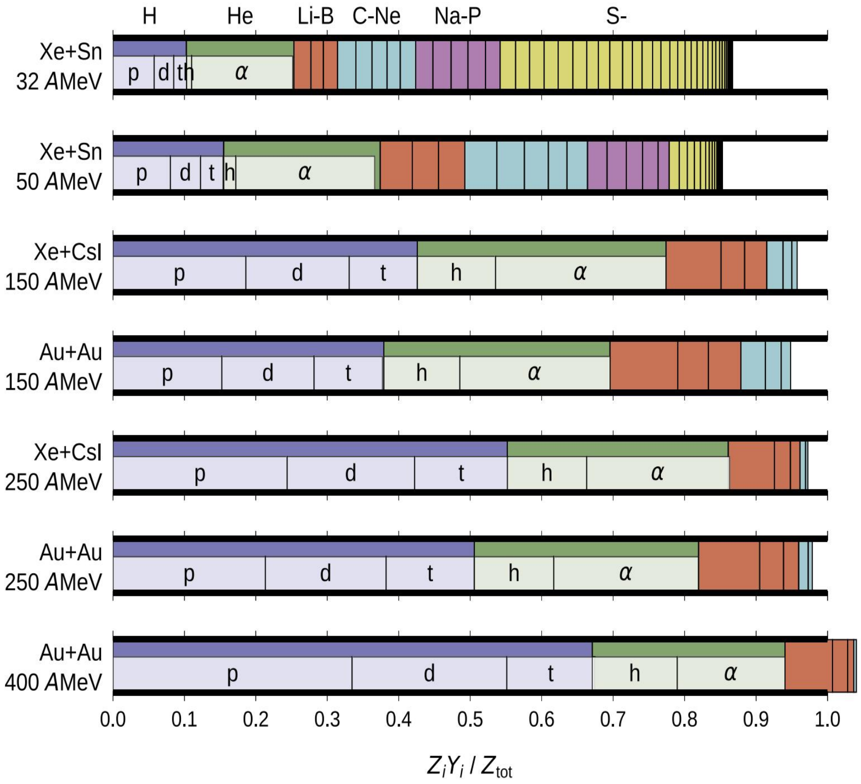

Clusters are produced by multinucleon or nucleon-cluster collisions

p+Λ+n+N↔${}_{\Lambda}^{3}$H+N′, p+Λ+n+n+N↔${}_{\Lambda}^{4}$H+N′, p+Λ+Λ+N↔${}_{\Lambda\Lambda}^{3}$H+N′, p+n+Λ+Λ+N ↔${}_{\Lambda\Lambda}^{4}$H+N′, p+p+Λ+N↔${}_{\Lambda}^{3}$He+N′, p+p+Λ+n+N↔${}_{\Lambda}^{4}$He+N′, p+p+Λ+Λ+N↔${}_{\Lambda\Lambda}^{4}$He+N′,

n+n+Λ+N↔${}_{\Lambda}^{3}$n+N′, n+n+Λ+Λ+N↔${}_{\Lambda\Lambda}^{4}$n+N′

以及π介子催化引起的反应道：

π+N_1+N_2↔π+deuteron, π+N_1+N_2+N↔deuteron+N′, π+N_1+N_2+N_3↔π+triton (helium-3), π+N_1+N_2+N_3+N→π+triton (helium-3)+N′, π+p+n+Λ↔π+${}_{\Lambda}^{3}$H, π+p+n+n +Λ↔π+${}_{\Lambda}^{4}$H, π+p+p+n+Λ↔π+${}_{\Lambda}^{4}$He

$$\frac{d\sigma}{d\Omega} = P(C_1 + C_2 \to C_3 + C_4) \times \frac{v_{\tilde{p}_{\rm rel}}}{v} \frac{\left|[\partial e(k)/\partial k]_{k=\tilde{p}_{\rm rel}}\right|}{\left|[\partial H(p_f)/\partial p_f]_{p_f=p_{\rm rel}}\right|} \frac{p_{\rm rel}^2}{\tilde{p}_{\rm rel}^2} \left[\frac{d\sigma_{NN}}{d\Omega}\right]_{\tilde{p}_{\rm rel}}$$

...

Schematic picture of nuclear cluster and hypercluster in HICs

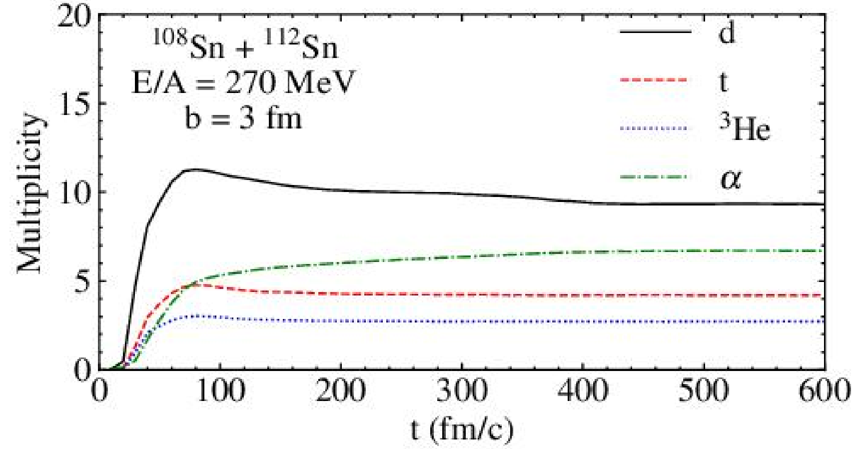

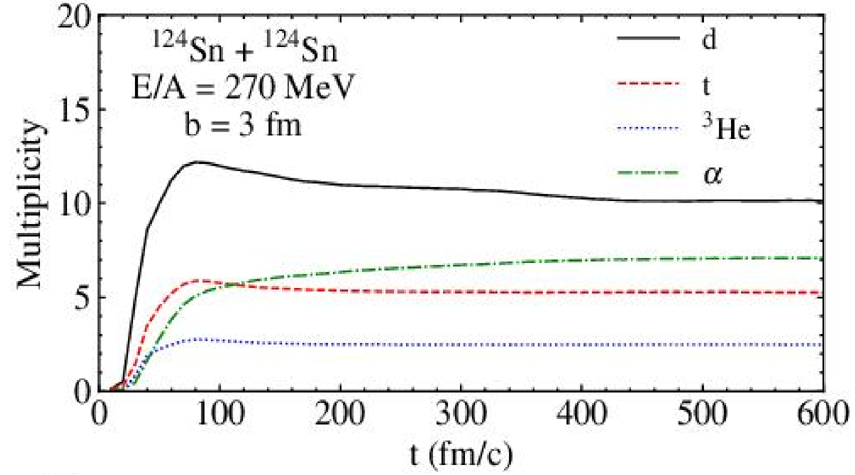

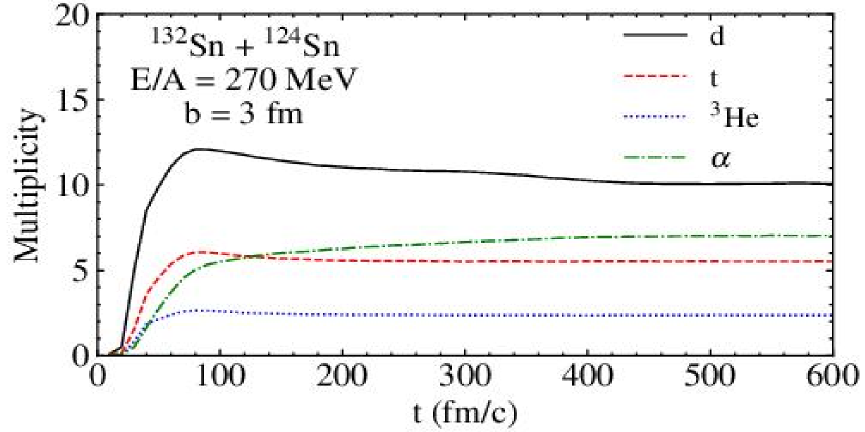

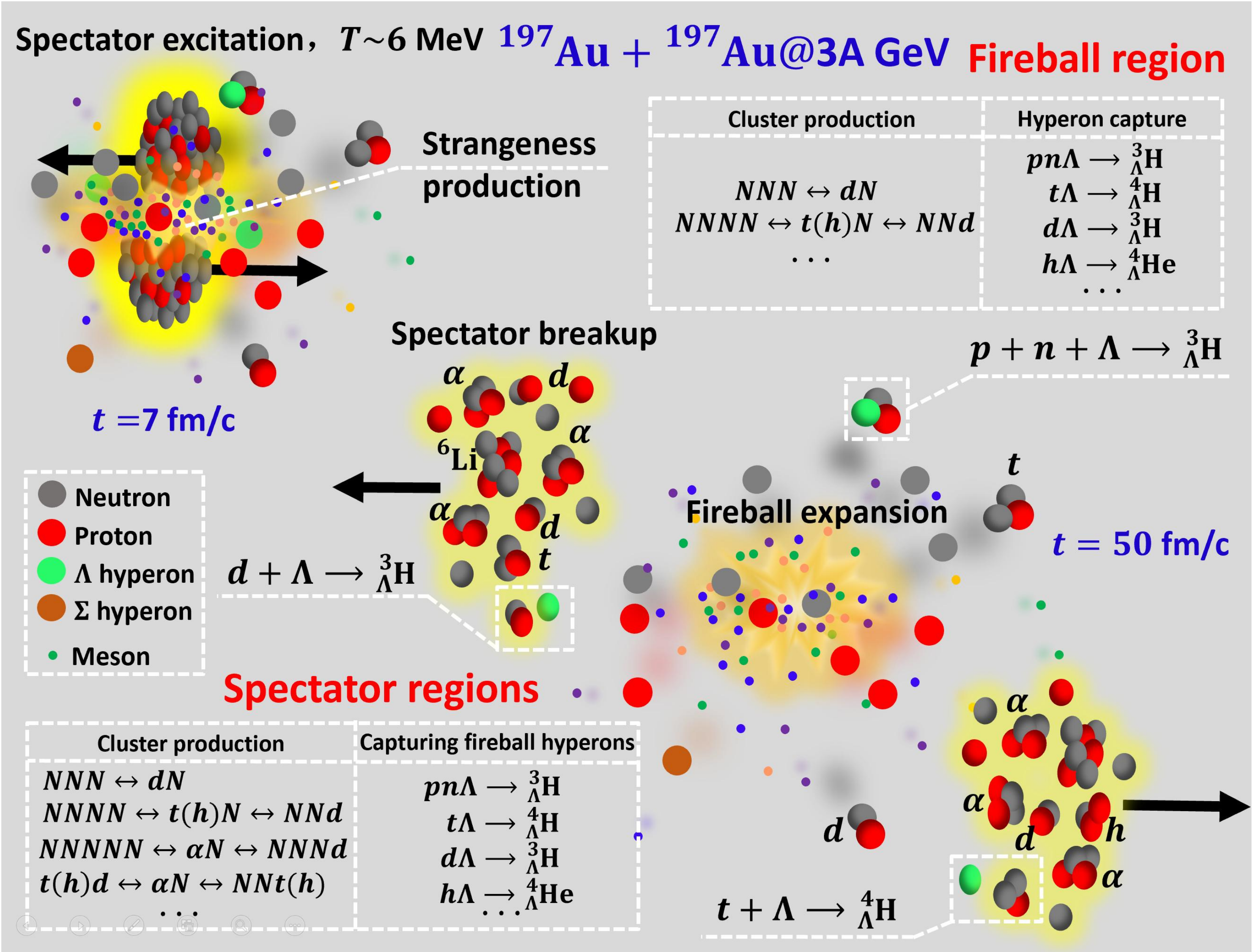

PHYSICAL REVIEW C **109**, L021602 (2024)

Letter

Kinetic approach for cluster production (LQMD.cluster)

Novel approach to light-cluster production in heavy-ion collisions

Hui-Gan Cheng and Zhao-Qing Feng*

School of Physics and Optoelectronics, South China University of Technology, Guangzhou 510640, China

(Received 8 November 2023; accepted 25 January 2024; published 15 February 2024)

$$
\begin{aligned}
H \quad &= \sum_i \frac{\mathbf{p}_i{}^2}{2m} + \frac{\alpha}{2}\sum_{\substack{i,j\\ j\neq i}} \frac{\rho_{ij}}{\rho_0} + \frac{\beta}{1+\gamma}\sum_i \left(\sum_{j,j\neq i} \frac{\rho_{ij}}{\rho_0}\right)^{\gamma} \\
&+ \frac{C_{sym}}{2}\sum_{\substack{i,j\\ j\neq i}} t_{z_i} t_{z_j} \frac{\rho_{ij}}{\rho_0} + \frac{g_{\rm sur}}{2}\sum_{\substack{i,j\\ j\neq i}}{}' \left[\frac{3}{2L} - \left(\frac{\mathbf{r}_i - \mathbf{r}_j}{2L}\right)^2\right] \frac{\rho_{ij}}{\rho_0} \\
&+ \sum_i^{N_C} E^i_{\rm z.p.} + \sum_i^{N_d} V_{\rm corr} e^{-r_i{}^2/4L}
\end{aligned}
$$

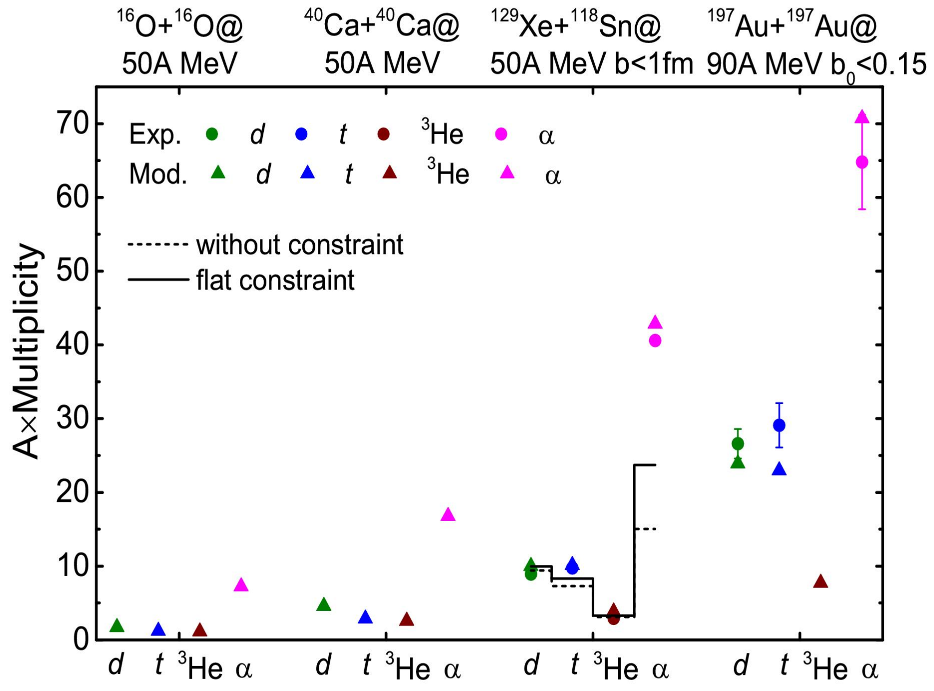

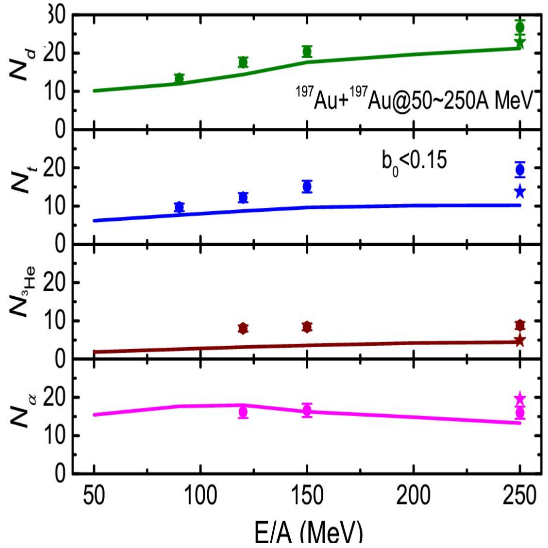

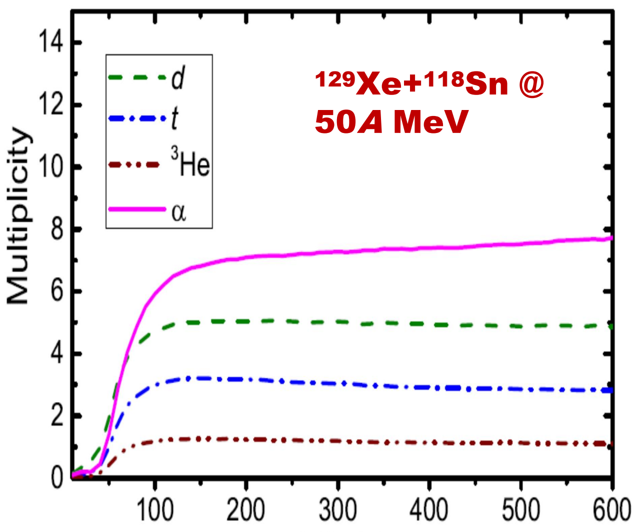

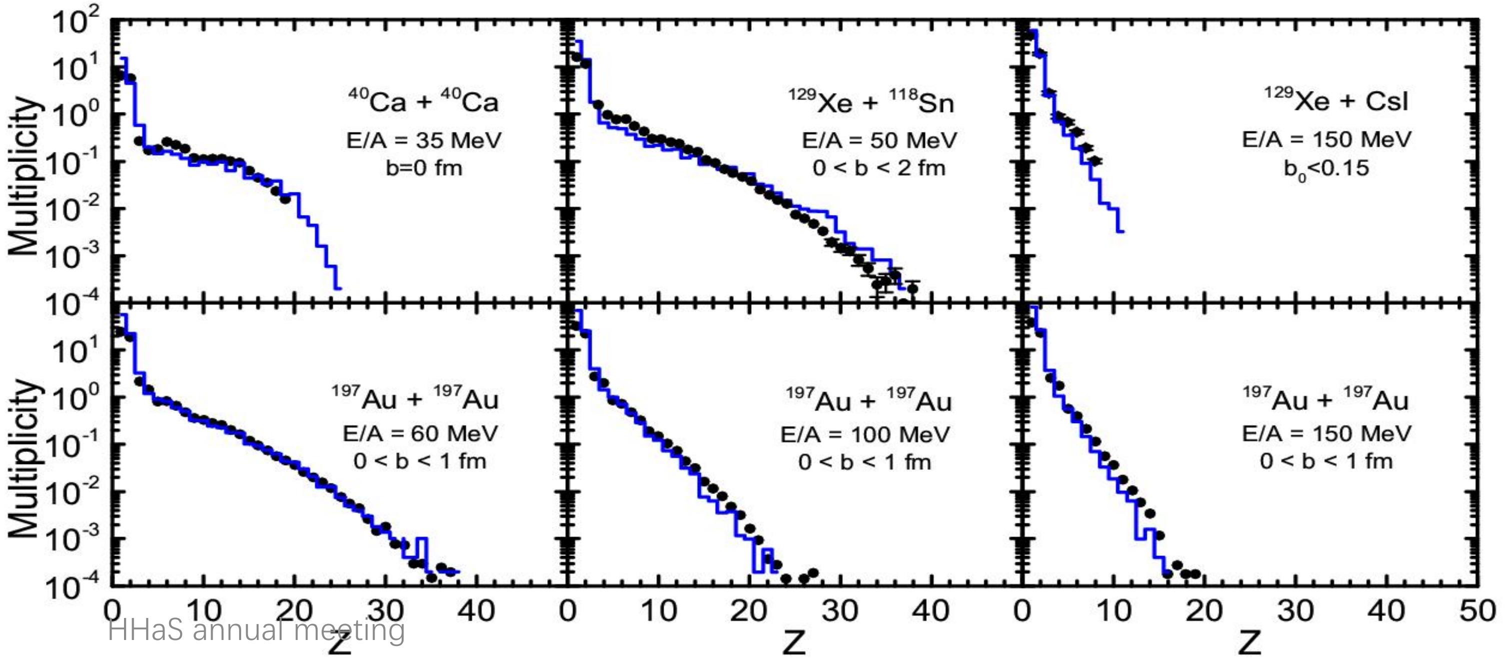

Collective flows of clusters in the isotopic nuclear reactions with a kinetic approach

Yuan-Qing Guo[1], Ban Zhang[1], Si-Min Chen[1], Hui-Gan Cheng[2], Ya-Peng Zhang[3], and Zhao-Qing Feng[1,3*]
[1] *School of Physics and Optoelectronics, South China University of Technology, Guangzhou 510640, China*
[2] *Guangdong University of Education, Guangzhou 510303, China*
[3] *State Key Laboratory of Heavy Ion Science and Technology, Institute of Modern Physics, Chinese Academy of Sciences, Lanzhou 730000, China*
(Dated: October 29, 2025)

Within the framework of Lanzhou quantum molecular dynamics transport model, the production of deuteron, triton, ^{3}He, and α in collisions of ^{132}Sn + ^{124}Sn, ^{124}Sn + ^{124}Sn and ^{108}Sn + ^{112}Sn at 270*A* MeV has been systematically investigated with a kinetic approach. It is demonstrated that the cluster production is correlated with the binding energy cluster potential, Mott effect etc, and the larger yields of deuteron and α in comparison with the triton and ^{3}He production. The mid-rapidity slope parameters of directed flows in the isotopic reactions increase with the mass number of cluster. The out-of-plane emission of protons is dominant in comparison with the cluster production and manifests the formation of compression nuclear matter. The emission timescale of clusters is correlated with the cluster formation in the cascade collisions and transportation in nuclear medium.

PACS number(s): 24.10.Lx, 25.70.Mn, 25.75.Ld
Keywords: Cluster production; Collective flows; Kinetic approach; LQMD transport model

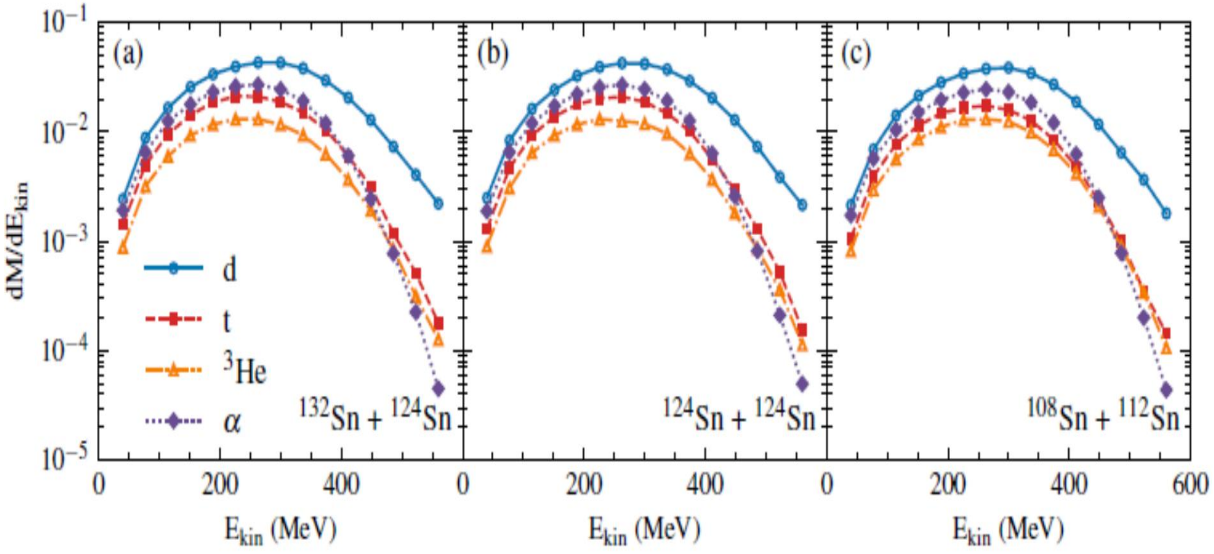

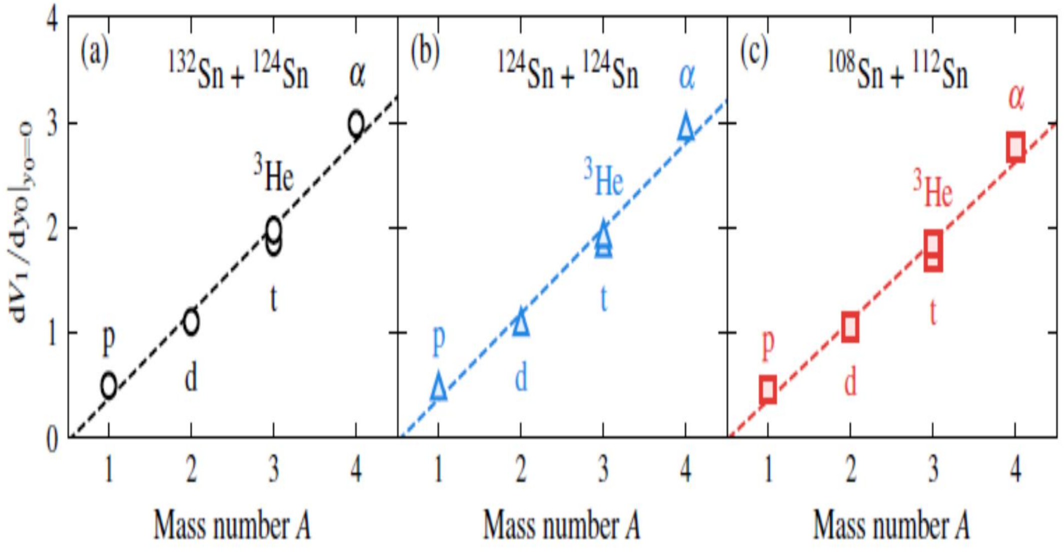

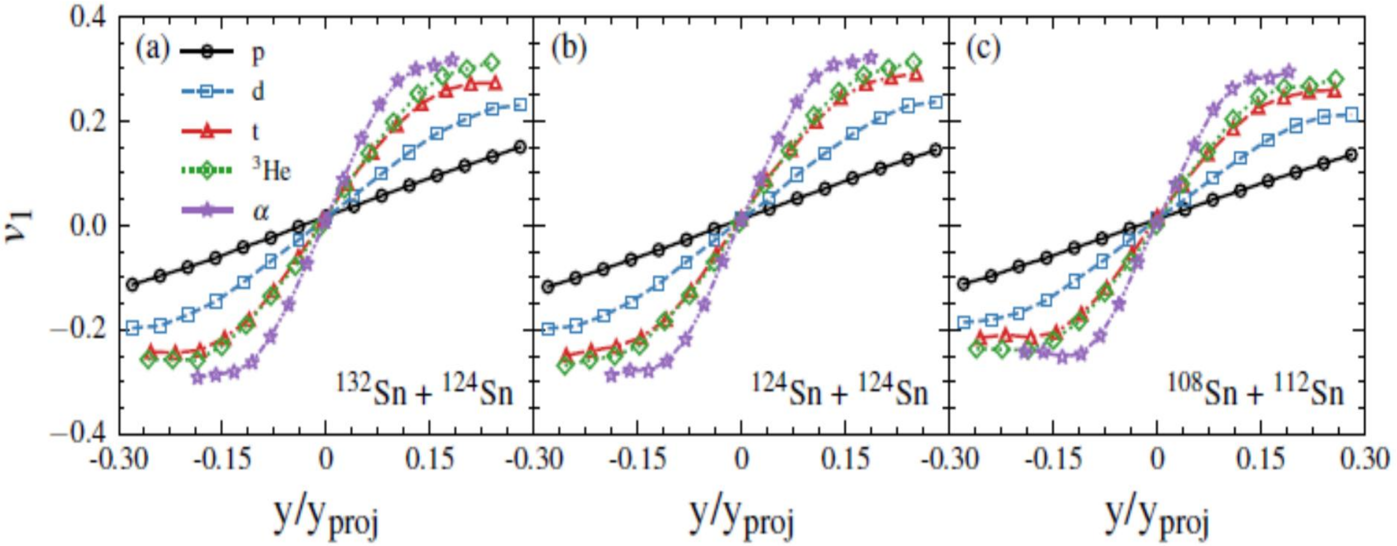

Hypernuclide production via HICs *(Wigner density approach)*

$^{124}Sn+^{124}Sn$@2*A* GeV

Z. Q. Feng, Phys. Rev. C 102, 044604 (2020)

Data: C. Rappold et al., (HypHI collaboration)
Phys. Lett. B 747, 129 (2015)

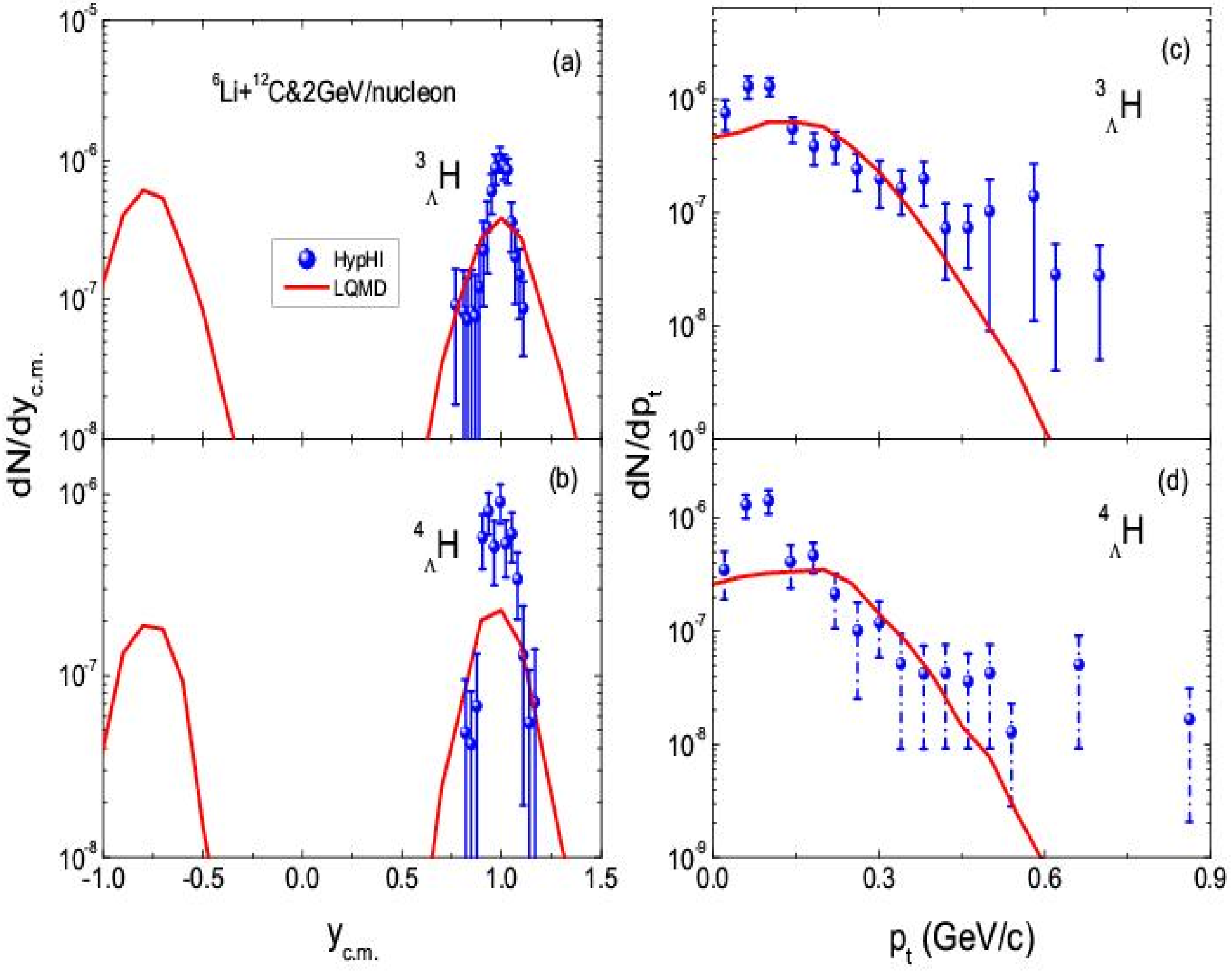

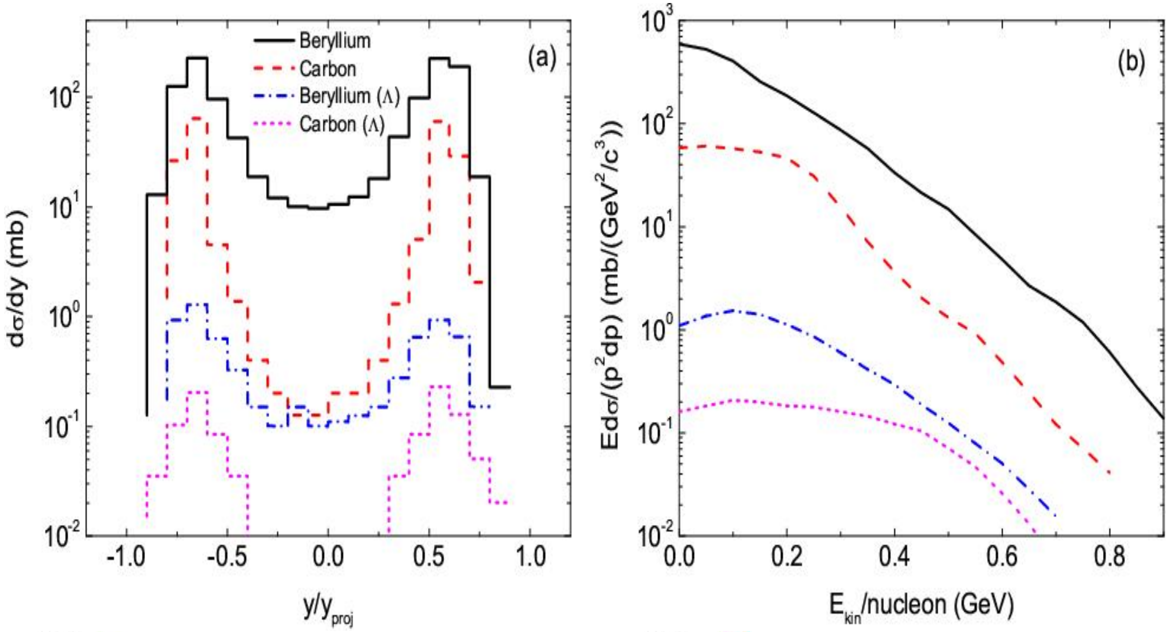

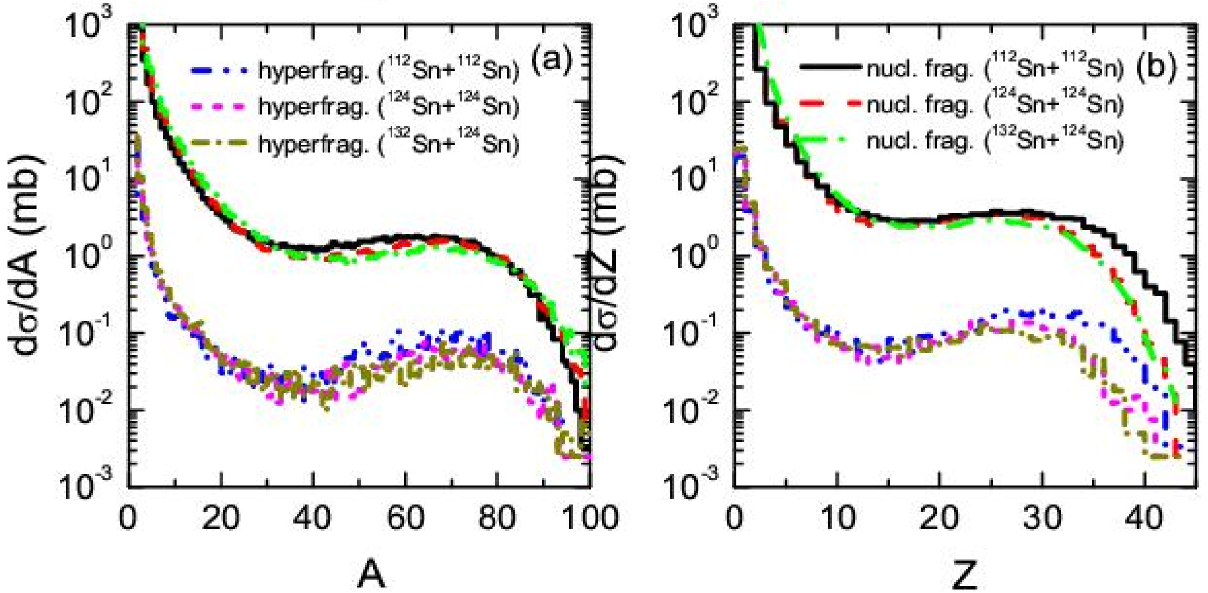

Multi-strangeness hypernuclide production

H.G. Cheng, Z. Q. Feng, Phys. Lett. B 824 (2022) 136849

^{197}Au+^{197}Au@3A GeV

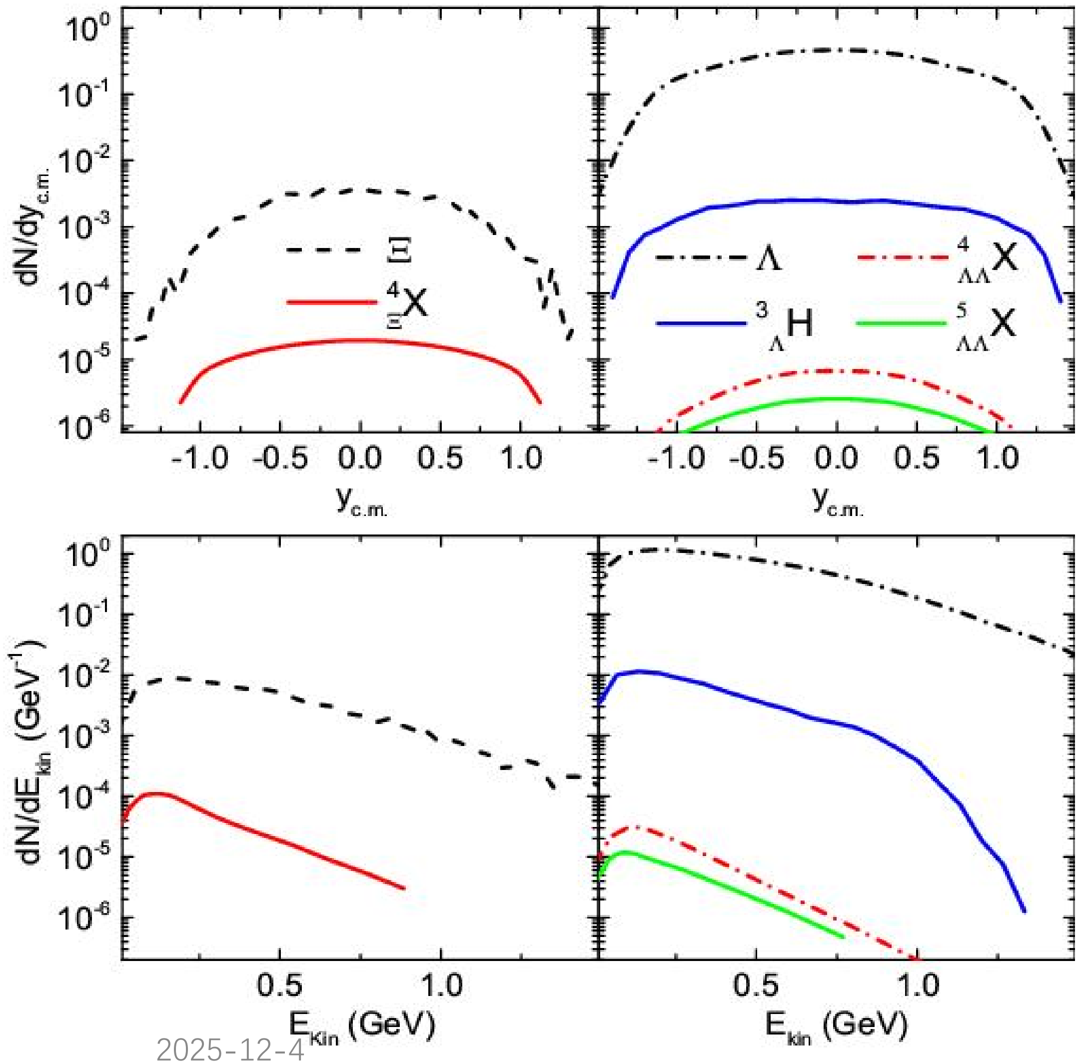

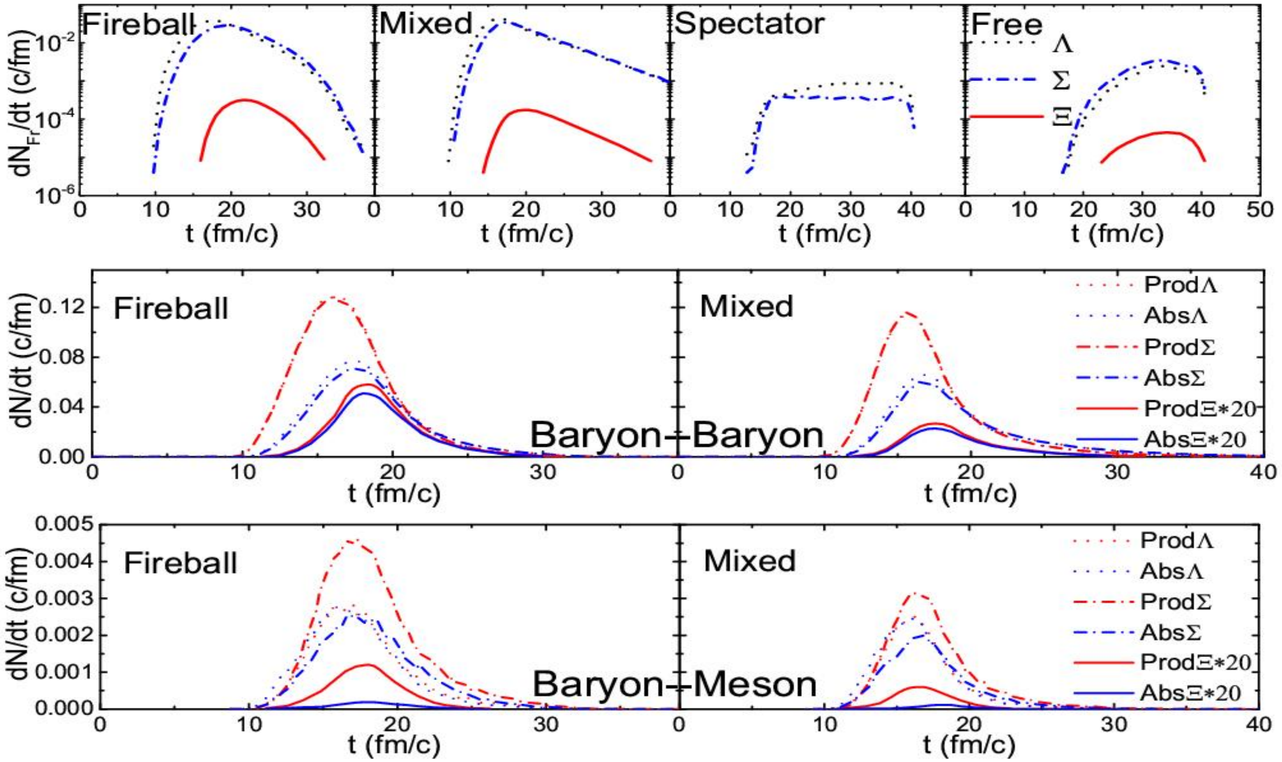

TABLE I. Comparison between cross sections of double lamda hypernuclei calculated with $r_0 = 3.5$ fm for Λ in ^{197}Au + ^{197}Au and ^{40}Ca + ^{40}Ca collisions at 3*A* GeV

Hypernuclei	Cross sections (mb)	
	^{197}Au + ^{197}Au	^{40}Ca + ^{40}Ca
$^{4}_{\Lambda\Lambda}$H	2.6×10^{-2}	1.0×10^{-4}
$^{4}_{\Lambda\Lambda}$He	1.0×10^{-2}	$\sim 10^{-5}$
$^{5}_{\Lambda\Lambda}$H	5.9×10^{-3}	$\sim 10^{-5}$
$^{5}_{\Lambda\Lambda}$He	5.1×10^{-3}	$\sim 10^{-5}$
$^{5}_{\Lambda\Lambda}$Li	1.4×10^{-3}	$\sim 10^{-6}$
$^{6}_{\Lambda\Lambda}$He	2.2×10^{-3}	$\sim 10^{-6}$
$^{7}_{\Lambda\Lambda}$He	6.8×10^{-4}	$\lesssim 10^{-6}$

IV. Summary

- The double charge exchange reactions in the pion induced reactions are particularly important for extracting the neutron-skin thickness of neutron-rich nuclei.
- The high-density symmetry probes single and double ratios of Σ^-/Σ^+(double ratio) via the isotopic reactions $^{112}Sn+^{112}Sn$ and $^{124}Sn+^{124}Sn$, in particular above 0.4 GeV.
- Hyperon production in heavy-ion collisions at HIAF energies provides a successful way for investigating the hyperon-nucleon potential in dense nuclear matter, e.g., ΛNN,ΣNN,ΞNN etc, might be constrained via heavy-ion collisions at HIAF.
- Kinetic approach is implemented in the LQMD transport model for the nuclear cluster production in Fermi energy heavy-ion collisions, hypercluster in the near future, in which the binding energy, multinucleon (cluster) collisions, Pauli principle, Mott effect etc are taken into account.

Thanks for your attention!

强流重离子加速器-HIAF

◻ 科学目标

集成离子超导直线加速器和环形同步加速器最先进的技术，**建造**一台束流指标先进、多学科用途的重离子科学综合研究装置—“强流重离子加速器研究装置”（HIAF），为核物理和核天体物理基础研究、原子物理、重离子束应用研究提供国际领先水平的实验平台。**基于HIAF，打造在国际上有重大影响的重离子科学研究中心**

总体方案：强流超导直线、快循环同步环、多实验终端结合